Identifying Monetary Policy Shocks by Matching Theoretical IRFs*

Myunghyun Kim† Sunho Lee‡ Inhwan So§

June 2026

Abstract

We propose a new structural vector autoregression (SVAR) identification scheme—the *matching restriction*—which exploits the information embedded in the impulse response functions (IRFs) derived from theoretical models. The matching restriction enables the empirical IRFs from SVARs to be close to the theoretical IRFs. In applications to monetary policy SVARs, we show that the matching restriction effectively addresses two well-known anomalies: the price puzzle and the positive output response to monetary tightening. Specifically, in an SVAR in which the price puzzle is present, the matching restriction based on the theoretical IRF of output (without matching price IRFs) eliminates the puzzle. Moreover, in an SVAR in which a contractionary monetary policy shock increases output, the matching restriction based on the theoretical IRF of prices (without matching output IRFs) allows the shock to decrease output. These findings clearly suggest that the matching restriction provides a bridge between structural theories and SVARs.

JEL Classification: C32, E31, E52, E58

Keywords: matching restriction; SVARs; monetary policy shocks; theoretical IRFs; sign restrictions; price puzzle

* We would like to thank Chaewon Baek, Minchul Shin, and the participants in the seminars at Sungkyunkwan University, Hongik University, and Bank of Korea for their helpful comments. The findings, interpretations, and conclusions expressed in this paper are entirely those of the authors and should not be attributed to the Bank of Korea. Kim acknowledges that this work was supported by the Ministry of Education of the Republic of Korea and the National Research Foundation of Korea (NRF-2022S1A3A2A01088457). All remaining errors are our own.

† Department of Economics, Sungkyunkwan University, Seoul, Korea (e-mail: mhkim7812@gmail.com).

‡ Bank of Korea, Seoul, Korea (e-mail: econ.preference@gmail.com).

§ School of Economics, Hongik University, Seoul, Korea (e-mail: inhwanso@hongik.ac.kr).

1 Introduction

Identifying monetary policy shocks in structural vector autoregressions (SVARs) is fundamentally an exercise that brings economic theory to data. Conventional identification schemes, however, have typically relied on only a limited subset of theoretical rationales. For instance, the recursive restriction in Christiano, Eichenbaum, and Evans (1996) assumes a specific timing of responses; that is, the monetary authority would respond contemporaneously to changes in economic activity and prices, but not to changes in monetary aggregates and reserves. This short-run restriction reflects the rationale of Taylor-type monetary policy rules in New Keynesian models. Another influential approach of Uhlig (2005) identifies monetary policy shocks by imposing a sign restriction that constrains the impulse response function (IRF) of prices to a contractionary monetary policy shock to fall for several months. This assumption is also based on a qualitative feature from a standard New Keynesian framework.

Whereas these conventional approaches are theoretically grounded to some extent, they are notably arbitrary or information-light as they focus only on the timing or the signs of the IRFs (Rudebusch, 1998; Baumeister and Hamilton, 2015). This partial reliance on theory (or theoretical models) may generate outcomes that are difficult to reconcile with theory, such as the price puzzle. That is, conventional restrictions use theory to justify lags or directions of the responses of some variables to specific shocks, yet discard other quantitative information from theoretical models, which may create a gap between the identified dynamics and the theory. Importantly, much of such information is inherently encapsulated within the IRFs derived from theoretical models (theoretical IRFs, hereafter). These IRFs quantitatively reflect the underlying structural channels and transmission mechanisms embedded in theoretical models. Put another way, the entire shape of a theoretical IRF—*inter alia*, its persistence, hump-shaped peaks or troughs, and decay—contains rich, high-dimensional information that conventional identification methods often fail to capture. Surprisingly, however, such theoretical IRFs have not yet been thoroughly used to impose restrictions in SVARs.

This paper bridges the gap by introducing a straightforward and intuitive identification scheme, the *matching restriction*. Unlike conventional approaches, the matching restriction fully employs the dynamic information implied by the theoretical IRFs. Formally, it uses the theoretical IRFs to construct a prior over the rotation matrix in SVARs, assigning higher prior density to rotations whose implied empirical IRF distributions are more compatible with the theoretical IRFs. This prior tilts posterior inference toward rotations whose implied empirical dynamics are more consistent with theory. By translating the theoretical IRF information into a prior distribution over rotations, our approach exploits the structural information from the underlying theoretical model.

We begin by describing the sign-restricted SVAR framework and the matching restriction

used throughout the paper. Specifically, we first derive the asymptotic posterior distribution of empirical IRFs conditional on the rotation matrix, and then use this distribution to assess how close the empirical IRFs are to the theoretical IRFs. If a rotation implies an empirical IRF distribution close to the theoretical IRFs, the corresponding density value under this distribution is high. The matching restriction uses this value to construct the prior over rotations, assigning more prior mass to rotations that are judged to generate empirical IRFs more similar to the theoretical IRFs.[1] Given the posterior distribution subject to both the sign restrictions and the matching restriction, we then describe the algorithm to draw from the distribution. The resulting posterior can be simulated by importance sampling, using draws from the sign-restricted posterior as proposals and the prior density over rotations as importance weights. This methodological alignment allows us to use the Bayesian estimation methods of Rubio-Ramírez, Waggoner, and Zha (2010) and Arias, Rubio-Ramírez, and Waggoner (2018) as the basis for posterior simulation.[2]

To obtain the theoretical IRFs, we construct a reference New Keynesian dynamic stochastic general equilibrium (DSGE) model. The model incorporates standard features of New Keynesian models, including nominal rigidities in prices and wages, habit formation in consumption, variable capital utilization, investment adjustment costs, etc. The monetary authority follows a Taylor-type monetary policy rule. As is typical in the related literature, a contractionary monetary policy shock leads to a hump-shaped decline in output and a persistent fall in prices in the model. The theoretical IRF of either output or prices to the shock in the model is used for the matching restriction to identify monetary policy shocks in SVARs.

With the theoretical IRFs from the DSGE model, we apply the matching restriction to two workhorse SVAR models: those of Arias, Caldara, and Rubio-Ramírez (2019) and Uhlig (2005). In the identification setup of Arias, Caldara, and Rubio-Ramírez (2019), which imposes the sign restrictions on the structural parameters, a contractionary monetary policy shock leads to a fall in output but fails to produce a significant decline in prices.[3] Surprisingly, however, after augmenting their SVAR model with a matching restriction based on the theoretical IRF of output, even without matching empirical and theoretical IRFs of prices, the shock decreases both output and prices—effectively resolving the price puzzle. Furthermore, in their SVAR model, the responses of commodity prices, nonborrowed reserves, and total reserves to the shock do not decrease and are close to zero. In contrast, the inclusion of the

[1] Since the conditional IRF distribution used for this evaluation depends on both the rotation and the data, the resulting prior over the rotation matrix has an empirical Bayes interpretation.

[2] This also ensures that our new restriction remains computationally compatible with state-of-the-art Bayesian inference.

[3] They also impose zero restrictions on the structural parameters. For simplicity, however, we first consider only their sign restrictions. It should be noted that the price puzzle persists even when both sign and zero restrictions are applied, as in their original identification setup. Nevertheless, Online Appendix E shows that the matching restriction can eliminate the puzzle when it is added to their sign and zero restrictions.

matching restriction yields significant decreases in them, a result consistent with economic theory.

The second application focuses on the SVAR framework of Uhlig (2005). Formally, this SVAR identifies monetary policy shocks by imposing a sign restriction on the IRFs of prices—a contractionary monetary policy shock cannot raise prices—to explicitly rule out the price puzzle, alongside sign restrictions on the federal funds rate, commodity prices, and nonborrowed reserves. That said, this setup leaves the IRF of output unconstrained, causing the notable anomaly that a contractionary monetary policy shock leads to an initial increase in output, inconsistent with standard theoretical predictions. To address this issue, we augment his SVAR model with a matching restriction based on the theoretical IRF of prices, without matching empirical and theoretical IRFs of output. We find that the inclusion of this additional information from the theoretical IRF of prices yields a significant negative output response after a monetary tightening shock, in line with theoretical expectations. These improvements collectively demonstrate the usefulness of the matching restriction in achieving a more precise and theory-consistent identification of monetary policy shocks.

We further show that the matching restriction significantly reduces identification uncertainty associated with monetary policy shocks in the above two applications. The improved results in the two applications are accompanied by tighter posterior IRF distributions. To explain, Giacomini and Kitagawa (2021) show that posterior uncertainty includes identification uncertainty generated by the non-unique rotation matrix and estimation uncertainty in the reduced-form parameters. Moreover, the matching restriction does not alter the reduced-form likelihood and prior and operates through the prior over rotations. Therefore, the compression of posterior IRF distributions mainly reflects a reduction in identification uncertainty over the rotation matrix.

This paper is related to several strands of the literature on identifying monetary policy shocks, proposing a method that renders the identification more consistent with macroeconomic theory. The first strand relies on timing and exclusion restrictions; e.g., the recursive scheme of Christiano, Eichenbaum, and Evans (1996) and its extension with the block exogeneity of Cushman and Zha (1997) (for a small open economy; Canada). While this approach is widely used by many researchers, straightforward to implement, and easy to estimate, it has been criticized for being somewhat arbitrary—imposing rigid delay assumptions that may not hold in theory and in reality. Empirically, these schemes often produce puzzling responses of key variables after a monetary policy shock, such as the price puzzle and delayed overshooting. Unlike the recursive restriction, our matching restriction does not impose timing assumptions, but instead uses theoretical IRFs to discipline the dynamic paths through the rotation prior.

The second strand is the literature on set-identification through sign and zero restric-

tions (Uhlig, 2005; Canova and Paustian, 2011; Arias, Caldara, and Rubio-Ramírez, 2019).[4] This approach provides greater flexibility than recursive ones by replacing rigid assumptions with qualitative directions based on related theory. However, from the perspective of set-identified SVARs, this flexibility raises the prior-dependence issue emphasized by Baumeister and Hamilton (2024). They argue that the way admissible rotations are weighted contains prior information and that its source should be made explicit. This paper contributes to this literature by providing one way to address this issue. Specifically, our matching restriction uses theoretical IRFs to construct an explicit, theory-based prior over the rotation matrix. Instead of relying solely on directional information, under the matching restriction, rotations that produce empirical IRFs closer to their corresponding theoretical IRFs are given higher prior density.

The third strand seeks identification through external information, including high-frequency changes in financial instruments (Gertler and Karadi, 2015; Jarociński and Karadi, 2020) and narrative records (Romer and Romer, 2004).[5] This approach has become increasingly popular as it avoids imposing arbitrary restrictions, while letting the data from outside the SVAR tell the story. However, it is data-driven by nature and thus rests heavily on the availability of specific, strong instruments. Our matching restriction shares a similar spirit in that it exploits information from outside the SVAR framework; yet, it departs substantially by using readily available theoretical information and bypassing the stringent data constraints.

The final strand is studies that attempt to exploit the theoretical information from DSGE models for SVAR analysis.[6] There are not many of these studies. For instance, Del Negro and Schorfheide (2004) use DSGE-implied population moments to construct priors for the reduced-form parameters of their SVAR. For structural identification, they use the rotation implied by the DSGE model, which need not be consistent with the finite-order SVAR approximation used to construct the prior. Liu and Theodoridis (2012) employ the DSGE-implied contemporaneous impact matrix in a penalty-function approach that deterministically selects one structural mapping that best approximates it. However, these approaches limit the selection of variables in SVAR models. Specifically, only the variables included in DSGE models can be used in SVAR models. Since nonborrowed reserves, total reserves, and commodity prices—which are important for identifying monetary policy shocks—are not typically

[4] As we apply the matching restriction to the sign-restricted SVAR frameworks, this literature is directly related to this paper.

[5] Kuttner (2001) also proposes a method to exploit monetary policy information, using the high-frequency changes in the short-term monetary instruments. Furthermore, to incorporate more information within the SVAR framework, Bernanke, Boivin, and Eliasz (2005) develop the factor-augmented VAR based on principal components.

[6] Besides these, there are many earlier studies on identifying monetary policy shocks. They include Romer and Romer (1989), Sims (1992), Christiano and Eichenbaum (1992), Bernanke and Blinder (1992), Strongin (1995), Rigobon and Sack (2004), etc.

included in DSGE models, they cannot be included in SVARs. In contrast, our matching restriction is much more flexible than these approaches because the matching restriction can be imposed even when only one variable in an SVAR model is included in a DSGE model.[7]

The paper proceeds as follows. Section 2 describes the details of the SVAR framework, explains the matching restriction, derives the posterior distribution, and presents the algorithm to draw from the distribution. Section 3 presents the theoretical IRFs of output and prices obtained from a New Keynesian DSGE model. Section 4 provides the main results of the SVARs with the matching restriction. Section 5 concludes the paper.

2 The matching restriction in the SVAR

In this section, we formalize our identification strategy by integrating the matching restriction—based on the theoretical IRFs from a New Keynesian DSGE model—into the standard SVAR framework. We begin by describing the SVAR framework for sign restrictions on the IRFs or the structural parameters and the matching restriction. We then derive and compare the specific forms of these two identifying restrictions. Finally, we derive the posterior distribution subject to both the sign and matching restrictions and explain the algorithm to draw from the distribution.

2.1 The SVAR model

We consider the following SVAR model:

$$\mathbf{Y}_t'\mathbf{A} = \sum_{j=1}^{p} \mathbf{Y}_{t-j}'\mathbf{C}_j + \boldsymbol{\alpha} + \boldsymbol{\varepsilon}_t', \tag{1}$$

where $\mathbf{Y}_t$ is an $n \times 1$ vector of endogenous variables, $\mathbf{A}$ and $\mathbf{C}_j$ are $n \times n$ parameter matrices, $\boldsymbol{\alpha}'$ is an $n \times 1$ vector of constants, and p is the lag length. $\boldsymbol{\varepsilon}_t$ is an $n \times 1$ vector of structural shocks, and its covariance matrix is $\mathbf{I}_n$, the $n \times n$ identity matrix. The sample size is T. Equation (1) can be rewritten more compactly as

$$\mathbf{Y}_t'\mathbf{A} = \mathbf{X}_t'\boldsymbol{\Gamma} + \boldsymbol{\varepsilon}_t', \tag{2}$$

[7] Since our identification method compares theoretical IRFs with empirical IRFs, it also has a natural connection to the IRF matching literature, which estimates DSGE parameters by making model-implied IRFs close to empirical IRFs from SVARs (e.g., Christiano, Eichenbaum, and Evans, 2005). Although the two approaches are methodologically related, they use IRFs for opposite purposes. Whereas the IRF matching uses empirical IRFs to estimate DSGE parameters, the matching restriction uses theoretical IRFs to construct a prior over the rotation matrix in a set-identified SVAR.

where $\mathbf{\Gamma}' = \left[\mathbf{C}_1', \cdots, \mathbf{C}_p', \boldsymbol{\alpha}'\right]$ is an $n \times m$ $(m = np + 1)$ matrix of parameters, and $\mathbf{X}_t' = \left[\mathbf{Y}_{t-1}', \cdots, \mathbf{Y}_{t-p}', 1\right]$ is a $1 \times m$ matrix for lagged endogenous variables and the constant term. The reduced-form representation of Equation (2) is

$$\mathbf{Y}_t' = \mathbf{X}_t'\mathbf{B} + \mathbf{u}_t' \tag{3}$$

with $\mathbf{B} = \mathbf{\Gamma}\mathbf{A}^{-1}$. $\mathbf{u}_t' = \boldsymbol{\varepsilon}_t'\mathbf{A}^{-1}$ is the vector of reduced-form innovations with covariance matrix $\mathbb{E}\left[\mathbf{u}_t\mathbf{u}_t'\right] = \left(\mathbf{A}\mathbf{A}'\right)^{-1} = \mathbf{\Sigma}$.

2.1.1 Empirical IRFs

Let $\mathbf{\Psi} = (\mathbf{A}, \mathbf{\Gamma})$ denote a collection of the structural parameter values. $\mathbf{IR}_h\left(\mathbf{\Psi}\right)$ is the matrix of impulse responses at horizon h, where the element in row i and column k represents the IRF of the i-th variable to the k-th structural shock. $\mathbf{IR}_h\left(\mathbf{\Psi}\right)$ can be formulated recursively as:

$$\begin{aligned}
\mathbf{IR}_0\left(\mathbf{\Psi}\right) &= \left(\mathbf{A}^{-1}\right)', \\
\mathbf{IR}_h\left(\mathbf{\Psi}\right) &= \sum_{j=1}^{h} \left(\mathbf{C}_j\mathbf{A}^{-1}\right)' \mathbf{IR}_{h-j}\left(\mathbf{\Psi}\right), \quad \text{for } 1 \leq h \leq p, \\
\text{and } \mathbf{IR}_h\left(\mathbf{\Psi}\right) &= \sum_{j=1}^{p} \left(\mathbf{C}_j\mathbf{A}^{-1}\right)' \mathbf{IR}_{h-j}\left(\mathbf{\Psi}\right), \quad \text{for } p < h < \infty.
\end{aligned}$$

It is noteworthy that the contemporaneous response ($\mathbf{IR}_0$) of the i-th variable to the k-th structural shock is directly determined by the (i,k)-th element of $\left(\mathbf{A}^{-1}\right)'$, one of the structural parameters. Hence, a sign restriction on the (i,k)-th element of $\left(\mathbf{A}^{-1}\right)'$ is equivalent to a restriction on the initial IRF of the i-th variable to the k-th structural shock.

2.1.2 Asymptotic posterior distribution of empirical IRFs

The matching restriction determines the prior density over the rotation matrix by evaluating the empirical IRF distribution implied by a rotation at the corresponding theoretical IRF. This distribution is obtained as the asymptotic posterior distribution of empirical IRFs. Here, we summarize the asymptotic posterior distribution whose detailed derivation is presented in Online Appendix A.

Let $\mathbf{Q} \in \mathcal{O}(n)$ be an $n \times n$ rotation matrix, where $\mathcal{O}(n) = \{\mathbf{Q} : \mathbf{Q}\mathbf{Q}' = \mathbf{I}_n\}$, and let $\mathbf{Y} = \left[\mathbf{Y}_1 \cdots \mathbf{Y}_T\right]'$ denote the sample. By the Bernstein-von Mises theorem, the posterior distribution of the reduced-form parameters, $\pi(\mathbf{B}, \mathbf{\Sigma} \mid \mathbf{Y})$, is asymptotically normal under standard regularity conditions (Vaart, 1998; Kleijn and Van Der Vaart, 2012). Also, since

empirical IRFs are functions of $\mathbf{B}$ and $\mathbf{\Sigma}$ given the rotation matrix $\mathbf{Q}$, the asymptotic normality of $\pi(\mathbf{B}, \mathbf{\Sigma} \mid \mathbf{Y})$ implies the asymptotic normality of the IRF distribution conditional on $\mathbf{Y}$ and $\mathbf{Q}$ (Lütkepohl, 1990). We refer to this conditional asymptotic IRF distribution as the $\mathbf{Q}$-conditional IRF distribution:

$$\begin{aligned} \mathbf{IR}^{(i,k)} \mid \mathbf{Y}, \mathbf{Q} &\overset{a}{\sim} \mathcal{N}\left(\boldsymbol{\mu}_Q^{(i,k)}(\mathbf{Y}), \mathbf{V}_Q^{(i,k)}(\mathbf{Y})\right) \\ \text{with } \boldsymbol{\mu}_Q^{(i,k)}(\mathbf{Y}) &= \mathbf{S}_{ik}\mathbf{IR}\left(\overline{\mathbf{B}}, \overline{\mathbf{\Sigma}}, \mathbf{Q}\right) \\ \text{and } \mathbf{V}_Q^{(i,k)}(\mathbf{Y}) &= \mathbf{S}_{ik}\mathbf{C}\left(\overline{\mathbf{B}}, \overline{\mathbf{\Sigma}}, \mathbf{Q}\right)\mathbf{\Omega}_{B,\Sigma}^{post}\mathbf{C}\left(\overline{\mathbf{B}}, \overline{\mathbf{\Sigma}}, \mathbf{Q}\right)'\mathbf{S}_{ik}'. \end{aligned} \tag{4}$$

$\mathbf{IR}(\cdot)$ is the stacked empirical IRF vector formed by stacking $\text{vec}(\mathbf{IR}_0(\cdot)), \ldots, \text{vec}(\mathbf{IR}_{H-1}(\cdot))$. $\mathbf{IR}^{(i,k)}$ is the empirical IRF vector of the i-th variable to the k-th structural shock over the matched horizons, and $\boldsymbol{\mu}_Q^{(i,k)}(\mathbf{Y})$ and $\mathbf{V}_Q^{(i,k)}(\mathbf{Y})$ are its $\mathbf{Q}$-conditional mean and covariance matrix, respectively. $\mathbf{S}_{ik}$ is the selection matrix that extracts this response from $\mathbf{IR}(\cdot)$. $\overline{\mathbf{B}}$ and $\overline{\mathbf{\Sigma}}$ are the posterior means of the reduced-form parameters, $\mathbf{\Omega}_{B,\Sigma}^{post}$ is their posterior covariance matrix, and $\mathbf{C}(\cdot)$ is the corresponding delta-method Jacobian.[8]

2.2 Prior distributions for identifying restrictions

Both sign and matching restrictions can be expressed in the form of prior distributions, but they operate in fundamentally different ways. For sign restrictions, the conventional approach assigns a uniform prior to the rotation matrix and then truncates the support of the parameter prior to the region in which the signs are satisfied. Rather than truncating the prior support, however, our matching restriction identifies structural shocks by assigning higher prior density to rotation matrices that are more compatible with the theoretical IRFs. Throughout this construction, the prior for the reduced-form parameters is kept separated from the matching restriction. This subsection derives and compares the specific forms of these two identifying restrictions.

2.2.1 Sign restriction

As shown in Rubio-Ramírez, Waggoner, and Zha (2010) and Arias, Rubio-Ramírez, and Waggoner (2018), the sign restrictions can be compactly expressed as the function:

$$\Upsilon(\mathbf{\Psi}) = \left(\mathbf{e}_{1,n}'\mathbf{F}(\mathbf{\Psi})'\mathbf{S}_1', \cdots, \mathbf{e}_{n,n}'\mathbf{F}(\mathbf{\Psi})'\mathbf{S}_n'\right)' > \mathbf{0}, \tag{5}$$

[8] These posterior moments should be computed from the unrestricted reduced-form posterior before truncation by the identifying restrictions.

where $\mathbf{e}'_{k,n}$ is the k-th column of the $n \times n$ identity matrix. $\mathbf{F}(\mathbf{\Psi})$ is a matrix that contains the candidate structural dynamics, and $\mathbf{S}_k$ is a selection matrix that isolates and signs the specific dimensions targeted for identification. The forms of $\mathbf{F}(\mathbf{\Psi})$ and $\mathbf{S}_k$ depend on whether the sign restrictions are imposed directly on the structural parameters or on the IRFs. For sign restrictions on the structural parameters, $\mathbf{F}(\mathbf{\Psi}) = \mathbf{\Psi}$, and $\mathbf{S}_k$ is an $s_k \times r_k$ matrix with elements $\{0, 1, -1\}$ which selects entries of $\mathbf{\Psi}$ over which r_k sign restrictions are imposed. For sign restrictions on the IRFs, $\mathbf{F}(\mathbf{\Psi})$ is the vertically stacked IRFs across different horizons, and $\mathbf{S}_k$ is an $s_k \times r_k$ matrix with elements $\{0, 1, -1\}$ which chooses the horizons and the variables over which the sign restrictions are imposed for the k-th structural shock.

Since the prior distributions should be written in terms of the reduced-form parameters, we need to reexpress the sign restrictions as a function of the reduced-form parameters. To do so, we reparameterize Equation (2) in terms of the reduced-form parameters ($\mathbf{B}$ and $\mathbf{\Sigma}$) and an orthogonal $n \times n$ matrix $\mathbf{Q} \in \mathcal{O}(n)$ as in Arias, Rubio-Ramírez, and Waggoner (2018) and Antolín-Díaz and Rubio-Ramírez (2018):

$$\mathbf{Y}'_t = \mathbf{X}'_t\mathbf{B} + \boldsymbol{\varepsilon}'_t\mathbf{Q}'R(\mathbf{\Sigma}), \tag{6}$$

where $R(\mathbf{\Sigma})$ is an $n \times n$ matrix with $R(\mathbf{\Sigma})' R(\mathbf{\Sigma}) = \mathbf{\Sigma}$. We use the Cholesky decomposition for $R(\cdot)$. Using $R(\cdot)$, we can define $f_R(\cdot)$ as a mapping between $\mathbf{\Psi}$ and $(\mathbf{B}, \mathbf{\Sigma}, \mathbf{Q})$:

$$f_R(\mathbf{\Psi}) = \Big(\underbrace{\mathbf{\Gamma}\mathbf{A}^{-1}}_{\mathbf{B}}, \underbrace{(\mathbf{A}\mathbf{A}')^{-1}}_{\mathbf{\Sigma}}, \underbrace{R\left((\mathbf{A}\mathbf{A}')^{-1}\right)\mathbf{A}}_{\mathbf{Q}}\Big) \tag{7}$$

$$\text{and } f_R^{-1}(\mathbf{B}, \mathbf{\Sigma}, \mathbf{Q}) = \Big(\underbrace{R(\mathbf{\Sigma})^{-1}\mathbf{Q}}_{\mathbf{A}}, \underbrace{\mathbf{B}R(\mathbf{\Sigma})^{-1}\mathbf{Q}}_{\mathbf{\Gamma}}\Big). \tag{8}$$

This invertible relationship allows us to transform the restrictions from the structural parameter space into the reduced-form domain. Using Equation (8), the sign restrictions in Equation (5) can be rewritten as a function of the reduced-form parameters and $\mathbf{Q}$ (i.e., $\Upsilon\left(f_R^{-1}(\mathbf{B}, \mathbf{\Sigma}, \mathbf{Q})\right)$), thereby acting to truncate the joint prior distribution over $(\mathbf{B}, \mathbf{\Sigma}, \mathbf{Q})$. Formally, the prior distribution under the sign restrictions takes the form:

$$[\![\Upsilon\left(f_R^{-1}(\mathbf{B}, \mathbf{\Sigma}, \mathbf{Q})\right) > 0]\!]\pi(\mathbf{B}, \mathbf{\Sigma}, \mathbf{Q}), \tag{9}$$

where $\pi(\mathbf{B}, \mathbf{\Sigma}, \mathbf{Q})$ denotes the joint prior density of the reduced-form parameters and $\mathbf{Q}$, and $[\![\cdot]\!]$ is an indicator function whose value is one when its argument is true and zero otherwise. When only sign restrictions are imposed, the prior distribution of $\mathbf{Q}$ is uniform under the Haar measure.

2.2.2 Matching restriction

The prior induced by the matching restriction ranks rotations based on how close the empirical IRF implied by each rotation is to the theoretical IRF.[9] Since the empirical IRF depends on the reduced-form parameters and $\mathbf{Q}$, we use the asymptotic posterior distribution of the reduced-form parameters to characterize the empirical IRF under each candidate rotation. As shown in Section 2.1.2, when $\mathbf{Q}$ is given, the asymptotic posterior distribution of the reduced-form parameters can be mapped directly into the $\mathbf{Q}$-conditional IRF distribution. This distribution represents the empirical IRF associated with a given rotation. A rotation therefore receives higher prior density when its conditional distribution assigns higher density to the theoretical IRF—which occurs when the empirical IRF under the rotation is closer to the theoretical IRF. Given that the $\mathbf{Q}$-conditional IRF distribution for constructing the prior over $\mathbf{Q}$ is derived from the data, the resulting prior has an empirical Bayes interpretation.

Although the $\mathbf{Q}$-conditional IRF distribution in Equation (4) is derived with the full covariance matrix $\mathbf{V}_Q^{(i,k)}(\mathbf{Y})$, we use a diagonalized covariance matrix to implement the matching restriction. This modification preserves the marginal uncertainty of each matched horizon while dropping the cross-horizon covariance terms. The resulting comparison evaluates the theoretical IRF on a horizon-by-horizon basis, rather than through covariance-induced linear combinations of IRF discrepancies whose economic interpretation is less transparent (Christiano, Trabandt, and Walentin, 2010). Specifically, to construct the prior over $\mathbf{Q}$, we use the following diagonalized $\mathbf{Q}$-conditional IRF distribution:

$$\mathbf{IR}^{(i,k)} \mid \mathbf{Y}, \mathbf{Q} \approx \mathcal{N}\left(\boldsymbol{\mu}_Q^{(i,k)}(\mathbf{Y}), \mathbf{D}_Q^{(i,k)}(\mathbf{Y})\right),$$

where $\mathbf{D}_Q^{(i,k)}(\mathbf{Y})$ denotes the diagonal matrix obtained by isolating the diagonal elements of $\mathbf{V}_Q^{(i,k)}(\mathbf{Y})$.

Let $\mathbb{IR}^{(i,k)}$ denote the theoretical IRF of the i-th variable to the k-th structural shock over the matched horizons. Then, evaluating the Gaussian density of the above distribution at $\mathbb{IR}^{(i,k)}$ gives a scalar function of $\mathbf{Q}$. We use this function as the prior density kernel:

$$m(\mathbf{Q}; \mathbf{Y}) = \phi_H\left[\mathbb{IR}^{(i,k)}; \boldsymbol{\mu}_Q^{(i,k)}(\mathbf{Y}), \mathbf{D}_Q^{(i,k)}(\mathbf{Y})\right], \tag{10}$$

where $\phi_H[\cdot; \boldsymbol{\mu}, \mathbf{D}]$ represents the H-dimensional Gaussian density with mean $\boldsymbol{\mu}$ and diagonal covariance matrix $\mathbf{D}$. Therefore, a rotation $\mathbf{Q}$ receives a larger value of $m(\mathbf{Q}; \mathbf{Y})$ when the theoretical IRF lies in a higher-density region of the diagonalized $\mathbf{Q}$-conditional IRF distribution. In this sense, the prior induced by the matching restriction assigns higher prior density

[9] Hereafter, for simplicity and practicality, we consider the case of the matching restriction for only one variable. It should also be noted that the matching restriction can easily be extended to multiple variables.

to rotations that generate empirical IRF distributions under which the theoretical IRF is more likely.

Furthermore, let $\mu_H(d\mathbf{Q})$ denote the Haar probability measure on $\mathcal{O}(n)$. We use μ_H as the reference measure on the rotation space; hence, all densities over $\mathbf{Q}$ in this subsection are understood with respect to μ_H. Normalizing the kernel $m(\mathbf{Q};\mathbf{Y})$ with respect to the Haar measure defines the rotation prior Π_Q through its density π_Q:

$$\pi_Q\left(\mathbf{Q} \mid \mathbf{Y}, \mathbb{IR}^{(i,k)}\right) \equiv \frac{d\Pi_Q}{d\mu_H}\left(\mathbf{Q} \mid \mathbf{Y}, \mathbb{IR}^{(i,k)}\right) = \frac{m(\mathbf{Q};\mathbf{Y})}{\int_{\mathcal{O}(n)} m(\widetilde{\mathbf{Q}};\mathbf{Y})\mu_H(d\widetilde{\mathbf{Q}})}. \tag{11}$$

Finally, the prior under the matching restriction is

$$\pi(\mathbf{B},\mathbf{\Sigma})\pi_Q\left(\mathbf{Q} \mid \mathbf{Y}, \mathbb{IR}^{(i,k)}\right), \tag{12}$$

where $\pi(\mathbf{B},\mathbf{\Sigma})$ denotes the prior density of the reduced-form parameters.

2.2.3 Discussion

The matching kernel $m(\mathbf{Q};\mathbf{Y})$ can be intuitively interpreted as a weighted distance between the theoretical and empirical IRFs with a penalty term. Specifically, since $\mathbf{D}_Q^{(i,k)}(\mathbf{Y})$ is diagonal, the log matching kernel can be reformulated, up to additive constants, as:

$$\log m(\mathbf{Q};\mathbf{Y}) = -\frac{1}{2}\left[\underbrace{\sum_{h=0}^{H-1}\frac{\left(\mathbb{IR}_h^{(i,k)} - \mu_{Q,h}^{(i,k)}(\mathbf{Y})\right)^2}{D_{Q,h}^{(i,k)}(\mathbf{Y})}}_{\text{Distance}} + \underbrace{\sum_{h=0}^{H-1}\log D_{Q,h}^{(i,k)}(\mathbf{Y})}_{\text{Penalty}}\right],$$

where $\mathbb{IR}_h^{(i,k)}$ is the h-th element of $\mathbb{IR}^{(i,k)}$, $\mu_{Q,h}^{(i,k)}(\mathbf{Y})$ is the h-th element of $\boldsymbol{\mu}_Q^{(i,k)}(\mathbf{Y})$, and $D_{Q,h}^{(i,k)}(\mathbf{Y})$ is the h-th diagonal element of $\mathbf{D}_Q^{(i,k)}(\mathbf{Y})$. Therefore, the log matching kernel can be decomposed into a distance term that measures the distance between the two IRFs and a penalty term for rotations that imply highly uncertain IRF distributions.

The distance term determines how discrepancies between the theoretical IRF and the mean of the $\mathbf{Q}$-conditional IRF distribution are weighted across horizons. At horizons where the empirical IRF is tightly estimated (i.e., $D_{Q,h}^{(i,k)}(\mathbf{Y})$ is small), even a relatively small discrepancy makes a larger contribution to the distance term, thereby lowering the prior density assigned to the rotation. In contrast, at horizons where the empirical IRF is imprecisely estimated, the same discrepancy has a smaller effect on the prior density.

Importantly, this weighting scheme reflects the purpose of the matching restriction. The matching restriction is not designed to force the empirical IRF to track the theoretical IRF at every horizon with equal strength. When the empirical IRF is precisely estimated at a given

horizon, the data provide sharper information about the dynamics implied by that rotation, and the theoretical IRF is allowed to discipline the rotation more strongly. When the empirical IRF is imprecisely estimated, the corresponding horizon provides weaker information for ranking rotations. Hence, the matching restriction assigns less weight to that part of the IRF path so that rotations are not incorrectly favored on the basis of noisy discrepancies.

The penalty term plays a different role. It prevents the matching restriction from favoring rotations that generate diffuse empirical IRF distributions. The prior density assigned to a rotation decreases through the penalty term when the variance of the **Q**-conditional IRF distribution implied by that rotation becomes large. This term also offsets the mechanical increase in prior density that could arise in the distance term when a large variance appears in the denominator. Hence, even if the theoretical IRF lies close to the mode of the **Q**-conditional IRF distribution, excessive uncertainty lowers the corresponding density value through the penalty term. The matching kernel favors rotations that bring the theoretical and empirical IRFs closer together without generating excessive uncertainty in the empirical IRF.

This decomposition shows why the matching restriction can compress the upper and lower bounds of posterior IRFs. Since posterior draws are reweighted by the matching kernel, rotations with a large distance term or a large penalty term receive small weights. These rotations either imply empirical IRFs far from the theoretical benchmark or generate highly uncertain IRF distributions, and thus tend to widen the upper and lower bounds of posterior IRFs. The matching restriction narrows these bounds by reducing the weight assigned to such rotations. Considering that posterior uncertainty consists of identification uncertainty due to the non-unique rotation matrix and estimation uncertainty in the reduced-form parameters (Giacomini and Kitagawa, 2021), and that the matching restriction operates through the prior over rotations without altering the reduced-form likelihood and prior, the bound compression reflects a reduction in identification uncertainty over the rotation matrix induced by the structure of the prior over rotations.

By reducing identification uncertainty over the rotation matrix, the matching restriction directly addresses a vulnerability of sign-restriction frameworks. Conventional sign restrictions are information-light because qualitative signs alone leave a large set of admissible rotations. This limitation often leads to excessively wide credible sets for empirical IRFs and renders posterior inference highly sensitive to the implicit choice of priors, yielding counter-intuitive empirical results (Baumeister and Hamilton, 2015; 2018).[10] Our matching restriction

[10] Baumeister and Hamilton (2024) raise a related but broader concern about the use of a uniform prior over the rotation matrix in set-identified SVARs. They argue that posterior inference about structural impulse responses in set-identified SVARs requires prior information over rotations and that the source of this information should be made explicit. The matching restriction addresses this concern by replacing an implicit reliance on a Haar-uniform density over rotations with an explicit, theory-based prior density grounded in

systematically addresses this lack of informativeness. Rather than relying solely on directional or qualitative constraints, our approach exploits the full quantitative information embedded in theoretical IRFs. Consequently, the matching restriction narrows down the identified set toward theory-consistent regions, thereby effectively mitigating the concerns of weak identification in set-identified SVAR models.

2.3 Bayesian inference

This subsection outlines the Bayesian framework used for posterior inference, building upon the methods of Rubio-Ramírez, Waggoner, and Zha (2010), Arias, Rubio-Ramírez, and Waggoner (2018), and Antolín-Díaz and Rubio-Ramírez (2018). We first set up the posterior distribution and its sampling algorithm without the matching restriction. We then introduce the matching restriction and describe the posterior distribution and sampling algorithm under both the sign restrictions and the matching restriction.

2.3.1 Posterior distribution without the matching restriction

We begin by describing the posterior distribution before imposing the matching restriction. For the reduced-form parameters $(\mathbf{B}, \mathbf{\Sigma})$, we use a conjugate normal-inverse-Wishart prior, $\mathcal{NIW}(\nu, \mathbf{\Phi}, \mathbf{S}, \mathbf{\Omega})$. Specifically, the conditional and marginal priors are given as:

$$\begin{aligned} \text{vec}(\mathbf{B}) \mid \mathbf{\Sigma} &\sim \mathcal{N}\left(\text{vec}(\mathbf{S}),\ \mathbf{\Sigma} \otimes \mathbf{\Omega}\right) \\ \text{and } \mathbf{\Sigma} &\sim \mathcal{IW}(\nu, \mathbf{\Phi}). \end{aligned}$$

In the empirical exercises, we use an improper, noninformative prior by setting ν, $\mathbf{\Phi}$, $\mathbf{S}$, and $\mathbf{\Omega}^{-1}$ equal to zero or zero matrices, following Arias, Caldara, and Rubio-Ramírez (2019).

Since the normal-inverse-Wishart prior is conjugate to the reduced-form VAR likelihood, the posterior distribution of $(\mathbf{B}, \mathbf{\Sigma})$ retains the closed-form representation (Arias, Rubio-Ramírez, and Waggoner, 2018):

$$(\mathbf{B}, \mathbf{\Sigma}) \mid \mathbf{Y} \sim \mathcal{NIW}(\hat{\nu}, \hat{\mathbf{\Phi}}, \hat{\mathbf{S}}, \hat{\mathbf{\Omega}}) \tag{13}$$

with $\hat{\nu} = T + \nu$, $\hat{\mathbf{\Omega}} = \left(\mathbf{X}'\mathbf{X} + \mathbf{\Omega}^{-1}\right)^{-1}$, $\hat{\mathbf{S}} = \hat{\mathbf{\Omega}}\left(\mathbf{X}'\mathbf{Y} + \mathbf{\Omega}^{-1}\mathbf{S}\right)$, $\hat{\mathbf{\Phi}} = \mathbf{Y}'\mathbf{Y} + \mathbf{\Phi} + \mathbf{S}'\mathbf{\Omega}^{-1}\mathbf{S} - \hat{\mathbf{S}}'\hat{\mathbf{\Omega}}^{-1}\hat{\mathbf{S}}$, and $\mathbf{X} = [\mathbf{X}_1 \ \cdots \ \mathbf{X}_T]'$.

Under the prior for the sign restrictions in Equation (9), the posterior distribution is obtained by truncating the posterior generated from Equation (13) to the region that satisfies the sign restrictions. This truncated posterior can be simulated by a standard acceptance–

theoretical IRFs.

rejection algorithm. Specifically, the sampling algorithm under the sign restrictions is as follows.

Algorithm 1: Sampling under sign restrictions *The following algorithm generates independent draws from the posterior distribution of* $(\mathbf{B}, \mathbf{\Sigma}, \mathbf{Q})$ *subject to the sign restrictions without imposing the matching restriction.*

(i) *Draw* $(\mathbf{B}, \mathbf{\Sigma})$ *independently from the normal-inverse-Wishart posterior in Equation* (13).

(ii) *Draw* $\mathbf{Q}$ *independently from the uniform distribution over* $\mathcal{O}(n)$.

(iii) *Check whether the sign restrictions are satisfied,* i.e. $[\![\Upsilon\left(f_R^{-1}(\mathbf{B}, \mathbf{\Sigma}, \mathbf{Q})\right) > 0]\!] = 1$. *If they are satisfied, proceed to step* (iv); *otherwise return to step* (i).

(iv) *Transform the draw* $(\mathbf{B}, \mathbf{\Sigma}, \mathbf{Q})$ *into the structural parameters using Equation* (8) *and save the structural draw. If the desired number of structural draws has been reached, stop; otherwise return to step* (i).

2.3.2 Posterior distribution with sign and matching restrictions

We now impose the matching restriction in addition to the sign restrictions. Combining the likelihood, the sign restriction, and the prior specified in Equations (11) and (12), the posterior distribution subject to both the sign restrictions and the matching restriction is characterized as:

$$\begin{aligned}\pi\left(\mathbf{B}, \mathbf{\Sigma}, \mathbf{Q} \mid \mathbf{Y}, \Upsilon, \mathbb{IR}^{(i,k)}\right) \propto & [\![\Upsilon\left(f_R^{-1}(\mathbf{B}, \mathbf{\Sigma}, \mathbf{Q})\right) > 0]\!] \\ & \times \pi(\mathbf{Y} \mid \mathbf{B}, \mathbf{\Sigma})\, \pi(\mathbf{B}, \mathbf{\Sigma})\, m(\mathbf{Q}; \mathbf{Y}).\end{aligned} \tag{14}$$

However, since direct sampling from this posterior is challenging, we use importance sampling. Specifically, the posterior under only the sign restrictions is used as the proposal distribution:

$$q(\mathbf{B}, \mathbf{\Sigma}, \mathbf{Q} \mid \mathbf{Y}, \Upsilon) \propto [\![\Upsilon\left(f_R^{-1}(\mathbf{B}, \mathbf{\Sigma}, \mathbf{Q})\right) > 0]\!]\, \pi(\mathbf{Y} \mid \mathbf{B}, \mathbf{\Sigma})\, \pi(\mathbf{B}, \mathbf{\Sigma}). \tag{15}$$

This proposal is the same as the distribution sampled by `Algorithm 1`. Combining Equations (14) and (15), we can obtain the importance ratio that is proportional to the matching kernel:

$$\frac{\pi\left(\mathbf{B}, \mathbf{\Sigma}, \mathbf{Q} \mid \mathbf{Y}, \Upsilon, \mathbb{IR}^{(i,k)}\right)}{q(\mathbf{B}, \mathbf{\Sigma}, \mathbf{Q} \mid \mathbf{Y}, \Upsilon)} \propto m(\mathbf{Q}; \mathbf{Y}). \tag{16}$$

Given a set of proposal draws $\{\mathbf{B}_s, \mathbf{\Sigma}_s, \mathbf{Q}_s\}_{s=1}^S$ from `Algorithm` 1, the normalized importance weight for each draw s is

$$w_s = \frac{\widetilde{w}_s}{\sum_{r=1}^S \widetilde{w}_r}, \tag{17}$$

where $\widetilde{w}_s = m\left(\mathbf{Q}_s; \mathbf{Y}\right)$ is the unnormalized importance weight.

The importance weight w_s has a direct interpretation. Draws receive larger importance weights when their rotations generate empirical IRF distributions that assign higher density to the theoretical IRF. Hence, the importance weights shift posterior mass toward rotations whose implied dynamics are closer to the theoretical IRF.

The posterior sampling procedure under both the sign restrictions and the matching restriction is summarized as follows.

Algorithm 2: Sampling under sign and matching restrictions *The following algorithm generates draws from the posterior distribution of* $(\mathbf{B}, \mathbf{\Sigma}, \mathbf{Q})$ *subject to both the sign restrictions and the matching restriction.*

(i) *Generate* S *proposal draws* $\{\mathbf{B}_s, \mathbf{\Sigma}_s, \mathbf{Q}_s\}_{s=1}^S$ *from* `Algorithm` 1.

(ii) *For each proposal draw, compute the matching kernel* $m\left(\mathbf{Q}_s; \mathbf{Y}\right)$ *using Equation* (10).

(iii) *Compute the importance weights* w_s *using Equation* (17).

(iv) *Resample from the proposal draws with probabilities* $\{w_s\}_{s=1}^S$.

(v) *Transform the resampled draws* $(\mathbf{B}, \mathbf{\Sigma}, \mathbf{Q})$ *into structural parameters using Equation* (8).

3 The theoretical IRFs

In this section, we build a reference New Keynesian DSGE model to derive the theoretical IRFs of output and prices following a contractionary monetary policy shock.

3.1 The New Keynesian DSGE model

The model features sticky prices and wages, habit formation in consumption, variable capital utilization, investment adjustment costs, etc. Moreover, the central bank conducts monetary policy according to a Taylor-type rule. Our model setup is similar to the New Keynesian DSGE models in Christiano, Eichenbaum, and Evans (2005) and Smets and Wouters (2007).

3.1.1 Final goods firm

The final goods firm uses the following technology to produce final goods, Y_t, by combining intermediate goods, $Y_t(i)$ for $i \in [0,1]$:

$$Y_t = \left(\int_0^1 Y_t(i)^{\frac{\varepsilon_p - 1}{\varepsilon_p}} di \right)^{\frac{\varepsilon_p}{\varepsilon_p - 1}}.$$

Accordingly, the demand function for the i-th intermediate good and the aggregate price index, P_t, are

$$Y_t(i) = \left(\frac{P_t(i)}{P_t} \right)^{-\varepsilon_p} Y_t$$
$$\text{and } P_t = \left(\int_0^1 P_t(i)^{1-\varepsilon_p} di \right)^{\frac{1}{1-\varepsilon_p}},$$

where $P_t(i)$ is the price of the i-th intermediate good.

3.1.2 Intermediate goods firms

Intermediate goods firms operate in a monopolistically competitive market and produce differentiated goods using the production function, given as:

$$Y_t(i) = A_t \hat{K}_t(i)^{\alpha} N_t(i)^{1-\alpha},$$

where A_t is a common productivity, $\hat{K}_t(i)$ is capital services of firm i, and $N_t(i)$ is labor input of firm i.

The firms face nominal rigidity as they are unable to adjust prices freely each period. Specifically, in each period, only a fraction $(1 - \theta_p)$ of firms can adjust their prices.

3.1.3 Labor packer

The labor packer combines differentiated household labor to produce final labor input, N_t, and sells final labor input to intermediate goods firms at the nominal wage, W_t. Household $h \in [0,1]$ supplies $N_t(h)$ units of labor at the nominal wage $W_t(h)$. The labor aggregation technology is given by

$$N_t = \left(\int_0^1 N_t(h)^{\frac{\varepsilon_w - 1}{\varepsilon_w}} dh \right)^{\frac{\varepsilon_w}{\varepsilon_w - 1}}.$$

The demand for labor of the household h and the aggregate wage index, W_t, are

$$N_t(h) = \left(\frac{W_t(h)}{W_t}\right)^{-\varepsilon_w} N_t$$
$$\text{and } W_t = \left(\int_0^1 W_t(h)^{1-\varepsilon_w} dh\right)^{\frac{1}{1-\varepsilon_w}}.$$

Similar to intermediate goods firms, households also face nominal rigidities in the form of Calvo-style wage stickiness. Specifically, in each period, a household optimally sets its nominal wage with a fixed probability of $(1-\theta_w)$.

3.1.4 Household

A typical household seeks to maximize its expected lifetime utility

$$\mathbb{E}_0 \sum_{t=0}^{\infty} \beta^t \left(\ln\left(C_t - bC_{t-1}\right) - \frac{N_t(h)^{1+\chi}}{1+\chi}\right),$$

subject to the nominal budget constraint:

$$\begin{aligned} P_t C_t + P_t I_t + B_{t+1} = & W_t(h) N_t(h) + (1+i_t) B_t + R_t^n K_t u_t \\ & - P_t \left(\chi_1 (u_t - 1) + \frac{\chi_2}{2}(u_t - 1)^2\right) \frac{K_t}{Z_t} + \Pi_t - P_t T_t, \end{aligned}$$

where C_t is aggregate consumption, I_t is investment, B_t is the stock of nominal bonds, i_t is the nominal interest rate, R_t^n is a nominal rental rate on capital services, K_t is physical capital, u_t is utilization, Z_t is the investment shock, Π_t is nominal profit distributed from firms, and T_t is a real lump sum tax/transfer from the government.

Physical capital evolves according to the law of motion:

$$K_{t+1} = (1-\delta) K_t + Z_t \left[1 - \frac{\tau}{2}\left(\frac{I_t}{I_{t-1}} - 1\right)^2\right] I_t.$$

3.1.5 Government and central bank

We assume that the government consumes an exogenous share of output, ω_t^g, in each period, and that the government balances its budget in each period:

$$G_t = \omega_t^g Y_t$$
$$\text{and } T_t = G_t.$$

The central bank sets the nominal interest rate according to an inertial Taylor-type rule:

$$i_t = (1-\rho_i)i + \rho_i i_{t-1} + (1-\rho_i)\left(\phi_\pi(\pi_t - \pi) + \phi_y(\ln Y_t - \ln Y_{t-1})\right) + \varepsilon_{i,t},$$

where $\pi_t \equiv P_t/P_{t-1} - 1$ is price inflation, variables without time subscript t denote their respective steady-state values, and $\varepsilon_{i,t}$ is a monetary policy shock.

Since we focus exclusively on the responses to monetary policy shocks, we do not explain other exogenous variables. One period in the model is one quarter, and the parameter values are summarized in Online Appendix B.

3.2 Theoretical IRFs to a monetary policy shock

The theoretical IRFs of output and prices to a contractionary monetary policy shock are shown in Figure 1. The shock is normalized to increase the annualized nominal interest rate by 25 basis points in the initial period.

In response to the shock, output exhibits a hump-shaped decline, peaking around three quarters after the shock before gradually reverting to its pre-shock level (left panel). This persistent and delayed response reflects the key features in our New Keynesian DSGE model. As is well-documented in the literature, habit formation in consumption and investment adjustment costs prevent an initial, sharp decline in private absorption, instead generating the observed hump-shaped dynamics. Together, the contractionary shock raises the real interest rate via the Taylor-type rule amid price stickiness, leading households to delay consumption.

The shock leads to a persistent decrease in prices (right panel). Under Calvo-type price and wage rigidities, firms and households cannot instantaneously adjust their nominal variables in response to the shock. Consequently, the aggregate price level declines gradually and persistently.

We use these theoretical IRFs of output and prices as the reference for our matching

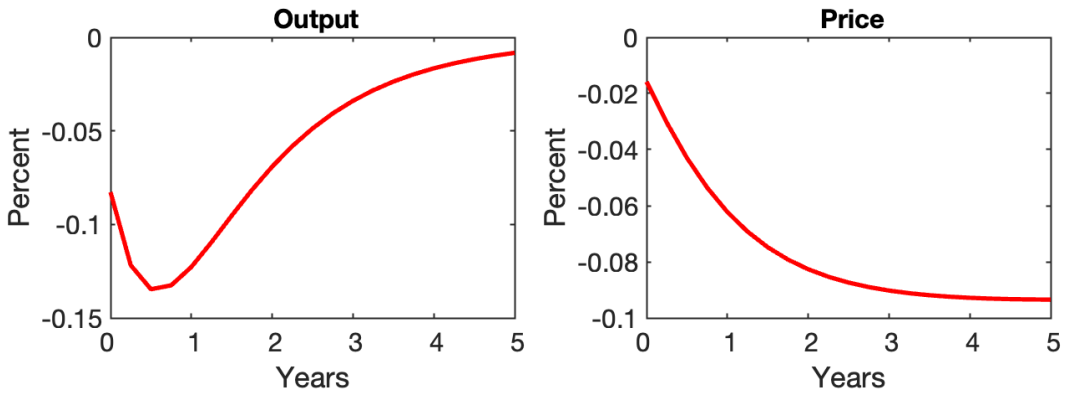

Figure 1: Theoretical IRFs of output and prices to a contractionary monetary policy shock

restriction to identify monetary policy shocks in the two SVARs in our applications. Specifically, in the SVAR in which the price puzzle is prevalent, we use only the theoretical IRF of output in the New Keynesian DSGE model to construct a prior over rotations that favors empirical output dynamics close to the theoretical benchmark. Then, we examine whether this prior distribution helps resolve the anomalous price response. On the other hand, in the SVAR in which output does not fall in response to a contractionary monetary policy shock, we use only the theoretical IRF of prices to construct the corresponding prior over rotations. Then, we check whether a contractionary monetary policy shock leads to a fall in output.

4 Results from the matching restriction

Using the theoretical IRF of either output or prices, this section applies the matching restriction to two workhorse SVARs of monetary policy analysis: those of Arias, Caldara, and Rubio-Ramírez (2019) and Uhlig (2005). We show that incorporating the theoretical benchmark through the matching restriction is highly effective in identifying monetary policy shocks.

4.1 The two monetary policy SVARs

The two SVAR models considered in this study face distinct identification challenges. In the SVAR of Arias, Caldara, and Rubio-Ramírez (2019) identified with sign and zero restrictions on the structural parameters, a contractionary monetary policy shock leads to a fall in output; however, the response of prices is not conclusive, failing to rule out the price puzzle. To address this, we augment their identification scheme with a matching restriction based on the theoretical IRF of output. Then, we evaluate whether the matching restriction helps resolve the price puzzle.

Meanwhile, in the SVAR of Uhlig (2005), prices fall after a contractionary monetary policy shock as the imposed sign restrictions rule out the price puzzle. Yet, the identified shock fails to produce a theoretically consistent decline in output. Accordingly, we add a matching restriction on the empirical and theoretical IRFs of prices to the identification scheme of Uhlig (2005). Then, we check whether the matching restriction leads to a contractionary response of output.

Data and others Following Arias, Caldara, and Rubio-Ramírez (2019) and Uhlig (2005), the SVAR models include six monthly US variables: real GDP, the GDP deflator, a commodity price index, total reserves, nonborrowed reserves, and the federal funds rate. We use the monthly real GDP and GDP deflator constructed by Arias, Caldara, and Rubio-Ramírez

(2019) via interpolation of the corresponding quarterly time series. The commodity price index is obtained from Global Financial Data, while total reserves, nonborrowed reserves, and the federal funds rate are sourced from the Federal Reserve Economic Data. All variables are seasonally adjusted except for the commodity price index and the federal funds rate. All variables are also logarithmic except for the federal funds rate. The lag length p is set to 12 months, as in Arias, Caldara, and Rubio-Ramírez (2019) and Uhlig (2005).

To exclude the structural shifts associated with the global financial crisis and the subsequent period of unconventional monetary policy, we limit the sample period from January 1965 to December 2007, as in Arias, Caldara, and Rubio-Ramírez (2019).

Finally, the DSGE model is quarterly, whereas the SVAR models are monthly. In addition, the shock sizes of the two differ. Therefore, we align the frequency of the empirical IRFs to quarterly and normalize the shock size in the SVAR models such that a contractionary monetary policy shock increases the federal funds rate by 25 basis points on impact, as in the DSGE model. We provide details of the frequency alignment and shock normalization procedures in Online Appendix C.

4.2 Matching the output responses

Here, we assess the effectiveness of the matching restriction in resolving the price puzzle within the SVAR framework of Arias, Caldara, and Rubio-Ramírez (2019). While their sign restrictions on the structural parameters provide a robust foundation for identifying monetary policy shocks, the resulting price responses exhibit the persistent price puzzle.

In this vein, we first consider the following sign restrictions on the structural parameters, identical to theirs.[11]

Sign Restriction 1: *The contemporaneous reaction of the federal funds rate, the monetary policy instrument, to output and prices is positive.*

`Sign Restriction` 1 implies that the central bank raises the federal funds rate in response to increases in output and prices. Consider the equation for the federal funds rate in the SVAR:

$$FF_t = \beta_G GDP_t + \beta_D DEF_t + \beta_C CP_t + \beta_T TR_t + \beta_N NBR_t + \sigma \varepsilon_{FF,t} + Others,$$

where FF, GDP, DEF, CP, TR, and NBR are the federal funds rate, real GDP, the GDP deflator, the commodity price index, total reserves, and nonborrowed reserves, respectively.

[11] Note that, different from Arias, Caldara, and Rubio-Ramírez (2019), we do not add zero restrictions for simplicity. The results in which zero restrictions are additionally imposed are shown in Online Appendix E.

The term *Others* includes the constant term, lagged variables, and other structural shocks. `Sign Restriction` 1 restricts the signs of β_G and β_D to be positive, which is consistent with the Taylor-type monetary policy rules in New Keynesian DSGE models.

As well-documented (Fry and Pagan, 2011; Baumeister and Hamilton, 2015), however, relying solely on sign restrictions like the one above is often insufficient for precise identification. Since sign restrictions only define a broad identified set of the structural parameters that satisfy the directional impact, they do not inherently rule out parameterizations that produce weak or even counter-intuitive dynamics, such as the price puzzle. Such an agnostic feature arises because the qualitative nature of sign restrictions lacks information regarding the quantitative magnitude and persistence of the responses.[12] The matching restriction, on the other hand, can complement this limitation by providing additional structural discipline. By assigning higher prior density to rotations that yield empirical dynamics more compatible with the theoretical IRFs, the matching restriction concentrates posterior mass on more theory-consistent dynamics, thereby facilitating a more robust identification of the monetary policy shock.

Taking these into account, we additionally consider a matching restriction based on the theoretical IRF of output that complements `Sign Restriction` 1 as follows:

Matching Restriction 1: *The closer the empirical IRF of GDP that a rotation yields is to the theoretical IRF of output and the lower the uncertainty of the empirical IRF of GDP is, the higher the prior density of the rotation.*

`Matching Restriction` 1 assigns higher prior density to rotations whose $\mathbf{Q}$-conditional IRF distributions for GDP are centered closer to the theoretical IRF of output in Figure 1. Equivalently, in Equation (10), $\mathbb{IR}^{(i,k)}$ is the theoretical IRF of output, and the matching kernel evaluates the density ϕ_H of the empirical IRF distribution of GDP at this theoretical IRF.

4.2.1 Results: Eliminating the price puzzle

We now present the results by comparing the IRFs identified under only the sign restrictions with those obtained by incorporating the matching restriction. The empirical IRFs under `Sign Restriction` 1 are computed from 2,000,000 draws, and these draws are resampled to incorporate `Matching Restriction` 1.[13] The monetary policy shock is normalized to raise the federal funds rate by 25 basis points on impact.

[12] Canova and Paustian (2011) demonstrate that, while sign restrictions can recover the directions of IRFs, they often fail to capture the structural dynamics beyond the initial impact horizon.

[13] The effective sample size implied by the importance weights is 1,039.8. The largest normalized weight is 0.48%.

Table 1: Distance between the empirical and theoretical IRFs of output

Restriction	`Sign Restriction` 1	`Sign Restriction` 1 & `Matching Restriction` 1
Posterior median	1.13	0.23
68% credible interval	[0.47, 3.74]	[0.14, 0.39]

Note: Figures summarize the posterior distribution of the Euclidean distance between the empirical and theoretical IRFs of output.

Table 1 illustrates how our approach improves identification by comparing the Euclidean distance between the empirical and theoretical IRFs of output across the two identification schemes. Under `Sign Restriction` 1 alone, the posterior median distance between the two IRFs is 1.13, with a wide 68% credible interval of [0.47, 3.74]. This broad dispersion reflects the agnostic nature inherent in the qualitative sign restrictions, as they admit a vast range of identified sets that are numerically consistent with the signs but dynamically distant from the theoretical IRF. When `Matching Restriction` 1 is additionally imposed, the posterior median distance falls to 0.23, and its 68% credible interval also shrinks to [0.14, 0.39]. This reduction in both the magnitude and the dispersion of the distance suggests that the matching restriction functions as a powerful informative prior.

Figure 2 plots the theoretical IRF of output (from the New Keynesian DSGE model; dashed line) and the corresponding empirical IRF of GDP (from the SVAR with the matching restriction; solid line) to a contractionary monetary policy shock. The figure demonstrates the successful alignment between the empirical and theoretical IRFs of output. Specifically, the median empirical IRF of GDP, identified through the matching procedure, closely tracks

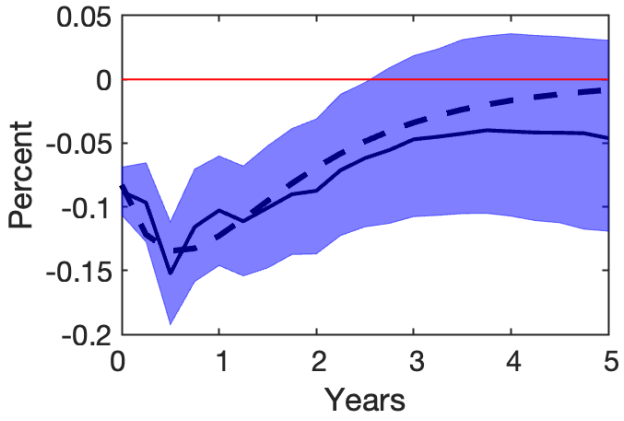

Figure 2: Empirical and theoretical IRFs of output to a monetary policy shock

Notes: The dashed line is the theoretical IRF of output in Figure 1. The shaded area and solid line are the 68 percent credible set and the median empirical IRF of GDP, respectively, using `Sign Restriction` 1 and `Matching Restriction` 1.

the hump-shaped path of the theoretical IRF. The fact that the 68% credible set (blue shaded area) is well-centered around the theoretical IRF confirms that `Matching Restriction 1` effectively recovers the structural dynamics of output implied by the theory. This provides a disciplined foundation for the subsequent analysis of other macroeconomic variables (including prices) that are not explicitly targeted by the matching procedure.

The effectiveness of the matching restriction is more evident in Figure 3, which compares the IRFs identified under only `Sign Restriction 1` (gray shaded area) and those under both `Sign Restriction 1` and `Matching Restriction 1` (blue shaded area). Under the sign restrictions alone, the response of the GDP deflator—the IRF of our primary interest in this exercise—to a contractionary monetary policy shock is inconclusive and fails to rule out the price puzzle, with the 68% credible set widening around zero throughout the horizon. Again, the wide credible set implies that the agnostic nature of the sign restrictions fails to provide enough information to pin down the price dynamics after the shock.

In contrast, the inclusion of `Matching Restriction 1` yields results that are more theoretically consistent. Upon imposing the matching restriction, the IRF of the GDP deflator to the shock exhibits a clear and persistent decline across all horizons, effectively resolving the price puzzle. Notably, the credible set becomes much tighter than that under only the sign restrictions. This narrowing, together with a clear decline, suggests that the matching restriction concentrates posterior mass on rotations that imply more theory-consistent dynamics.

As in Figure 2, which shows how the matching restriction disciplines the empirical IRF of GDP toward its corresponding theoretical IRF, the comparison between the two empirical IRFs of GDP in Figure 3 reconfirms the effectiveness of our approach. While `Sign Restriction 1` alone already produces a negative median path, the inclusion of the matching restriction results in a substantially narrower credible set. This demonstrates that the matching restriction does not merely incorporate the direction of the response but effectively exploits the full quantitative information embedded in the theoretical IRF of output.

Furthermore, this feature of the matching restriction extends to the IRF of commodity prices. Under only `Sign Restriction 1`, the median IRF of commodity prices is negative. However, its 68% credible set includes the zero line over the horizon. In contrast, with `Matching Restriction 1`, the IRF is significantly negative over the horizon, reaching its trough around one year after the shock. This suggests that by identifying the output dynamics in a more theory-consistent manner, the SVAR better captures the decline in aggregate demand and the subsequent downward pressure on commodity prices, which is consistent with existing studies such as Kim (2022).

Regarding the policy-related reserve variables, total reserves and nonborrowed reserves, the matching restriction also yields clearer contractionary responses than those under only

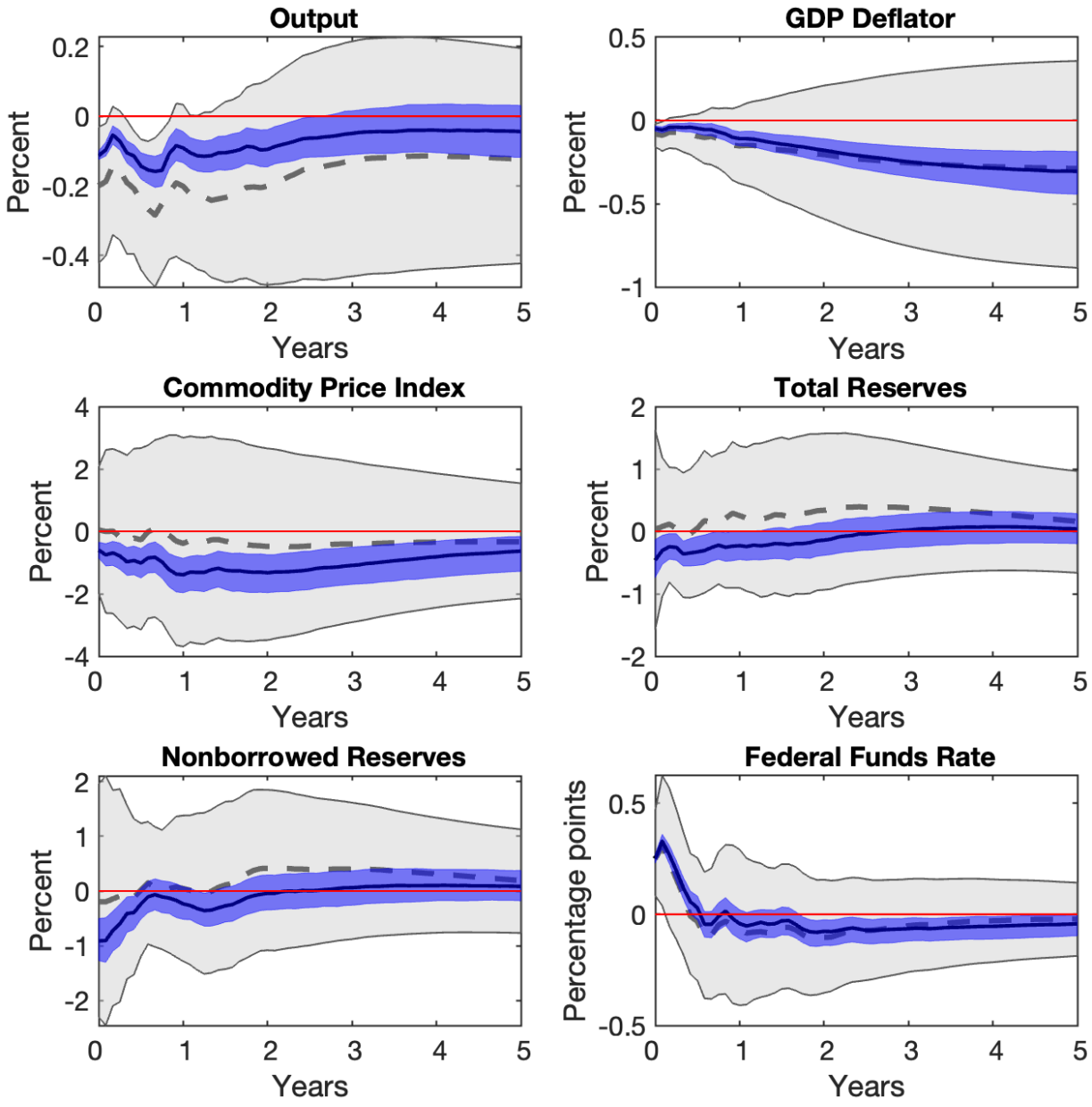

Figure 3: IRFs to a monetary policy shock (`Sign Restriction` 1 & `Matching Restriction` 1)

Notes: The lighter shaded areas and dashed lines are the 68 percent credible sets and the median IRFs, respectively, using `Sign Restriction` 1. The darker shaded areas and solid lines are the 68 percent credible sets and the median IRFs, respectively, using `Sign Restriction` 1 and `Matching Restriction` 1.

`Sign Restriction 1`. With `Matching Restriction 1`, total reserves become significantly negative for about eight months after the shock, while nonborrowed reserves are significantly negative for roughly six months. The application of the matching restriction also leads to a noticeable reduction in the width of their credible sets.

As discussed in Section 2.2.3, the matching restriction leads to a large reduction in identification uncertainty over the rotation matrix in this application. The narrower credible sets of the variables in Figure 3 clearly reveal this feature. To examine this more directly, we further compare the upper and lower bounds of posterior IRF samples before and after applying `Matching Restriction 1` in Online Appendix D. The results collectively show that the bounds become far more compressed after the matching restriction is incorporated.

4.3 Matching the responses of prices

We shift our focus to the effectiveness of the matching restriction within the SVAR framework of Uhlig (2005). He originally adopted sign restrictions on price responses to avoid the price puzzle. However, his identification creates another puzzle: A contractionary monetary policy shock does not decrease output, which is inconsistent with economic theory. To address this, we incorporate a matching restriction based on the theoretical IRF of prices into Uhlig's (2005) framework to examine whether the matching restriction can improve the identification of output dynamics.

Formally, we employ the following sign restrictions on the IRFs:

Sign Restriction 2: *A contractionary monetary policy shock decreases the GDP deflator, the commodity price index, and nonborrowed reserves but increases the federal funds rate for six months after the shock.*

`Sign Restriction 2` is the same as that used in Uhlig (2005). These restrictions rule out the price puzzle by construction. However, it remains intentionally agnostic about the response of output.

Besides this qualitative approach, we additionally consider a matching restriction which makes use of the quantitative information from the theoretical IRF of prices in the New Keynesian DSGE model:

Matching Restriction 2: *The closer the empirical IRF of the GDP deflator that a rotation yields is to the theoretical IRF of prices and the lower the uncertainty of the empirical IRF of the GDP deflator is, the higher the prior density of the rotation.*

`Matching Restriction 2` assigns higher prior density to rotations whose $\mathbf{Q}$-conditional IRF

Table 2: Distance between the empirical and theoretical IRFs of prices

Restriction	`Sign Restriction 2`	`Sign Restriction 2` & `Matching Restriction 2`
Posterior median	1.33	0.26
68% credible interval	[0.44, 3.77]	[0.13, 0.51]

Note: Figures summarize the posterior distribution of the Euclidean distance between the empirical and theoretical IRFs of prices.

distributions for the GDP deflator are centered closer to the theoretical IRF of prices in Figure 1. Equivalently, in Equation (10), $\mathbb{IR}^{(i,k)}$ is the theoretical IRF of prices, and the matching kernel evaluates the density ϕ_H of the empirical IRF distribution of the GDP deflator at this theoretical IRF. By matching the empirical and theoretical IRFs of prices in this way, the restriction aims to sharpen the identification of the remaining macroeconomic variables, particularly output, whose response is puzzling under the original sign restrictions of Uhlig (2005).

4.3.1 Results: Resolving the puzzling response of output

We report the empirical results for the SVAR of Uhlig (2005), focusing on whether the matching restriction can lead to a decline in output in response to a contractionary monetary policy shock. As in the previous exercise, we contrast two identification schemes: one relying solely on `Sign Restriction 2` and the other incorporating both `Sign Restriction 2` and `Matching Restriction 2`. Specifically, the empirical IRFs under `Sign Restriction 2` are computed from 400,000 draws, which are resampled to incorporate `Matching Restriction 2`.[14] Also, the monetary policy shock is normalized to raise the federal funds rate by 25 basis points on impact.

Table 2 presents the comparison of the Euclidean distances between the empirical and theoretical IRFs of prices across the two identification schemes. Similar to our previous findings, the incorporation of the matching restriction facilitates a remarkable gain in consistency with the theoretical dynamics. The posterior median distance, which stands at 1.33 under the sign-restriction-alone scheme, falls to 0.26 when the matching restriction is added. Moreover, the 68% credible interval contracts from [0.44, 3.77] to [0.13, 0.51]. Again, this improvement reflects the fact that the matching restriction assigns greater posterior mass to rotations that are more compatible with the theoretical price dynamics.

[14] The effective sample size implied by the importance weights is 1,096.5. The largest normalized weight is 0.44%.

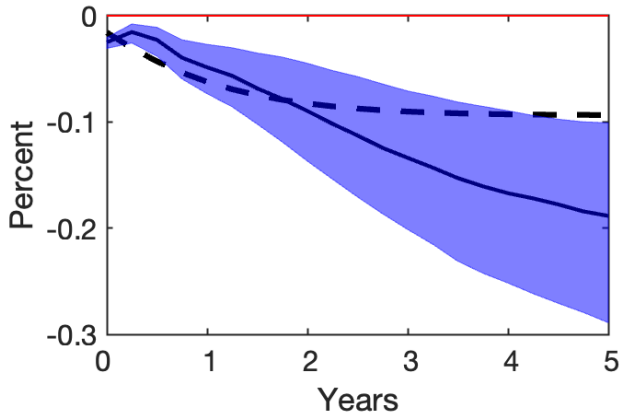

Figure 4: Empirical and theoretical IRFs of prices to a monetary policy shock

Notes: The dashed line is the theoretical IRF of prices in Figure 1. The shaded area and solid line are the 68 percent credible set and the median empirical IRF of the GDP deflator, respectively, using `Sign Restriction` 2 and `Matching Restriction` 2.

In Figure 4, we compare the empirical IRF of the GDP deflator, identified through the matching procedure, with the theoretical IRF of prices. The median empirical IRF of prices (solid line) closely tracks the theoretical benchmark (dashed line); both gradually fall after a monetary tightening shock. In addition, the credible set (blue shaded area) encompasses the theoretical IRF quite well, implying that `Matching Restriction` 2 aligns the empirically identified set with the structural dynamics of prices suggested by theory. This provides a foundation for analyzing the IRFs of the other variables, most notably output.

We report the IRFs to a contractionary monetary policy shock in Uhlig's (2005) SVAR in Figure 5, comparing those under the two distinct schemes: (*i*) `Sign Restriction` 2 alone (dashed lines and gray shaded areas) and (*ii*) `Sign Restriction` 2 and `Matching Restriction` 2 (solid lines and blue shaded areas). Among them, the IRF of GDP is positive to the shock, which is inconsistent with theory, under only `Sign Restriction` 2, and its 68% credible set is excessively wide. However, once `Matching Restriction` 2 is adopted, the GDP IRF becomes distinctly negative, with its credible set excluding the zero line around half a year after the shock. This suggests that, by exploiting the information from the theoretical IRF of prices, the matching restriction helps contractionary monetary policy shocks be contractionary, indeed.

Similar to our previous exercise, the matching restriction also yields enhanced posterior precision for other variables. Specifically, the credible sets for the IRFs of commodity prices, total reserves, and nonborrowed reserves to a contractionary monetary policy shock are all narrower when both `Sign Restriction` 2 and `Matching Restriction` 2 are imposed than when only `Sign Restriction` 2 is used.

Again, the narrower credible sets of the variables stem from the reduced identification uncertainty over the rotation matrix, thanks to the matching restriction. Specifically, the

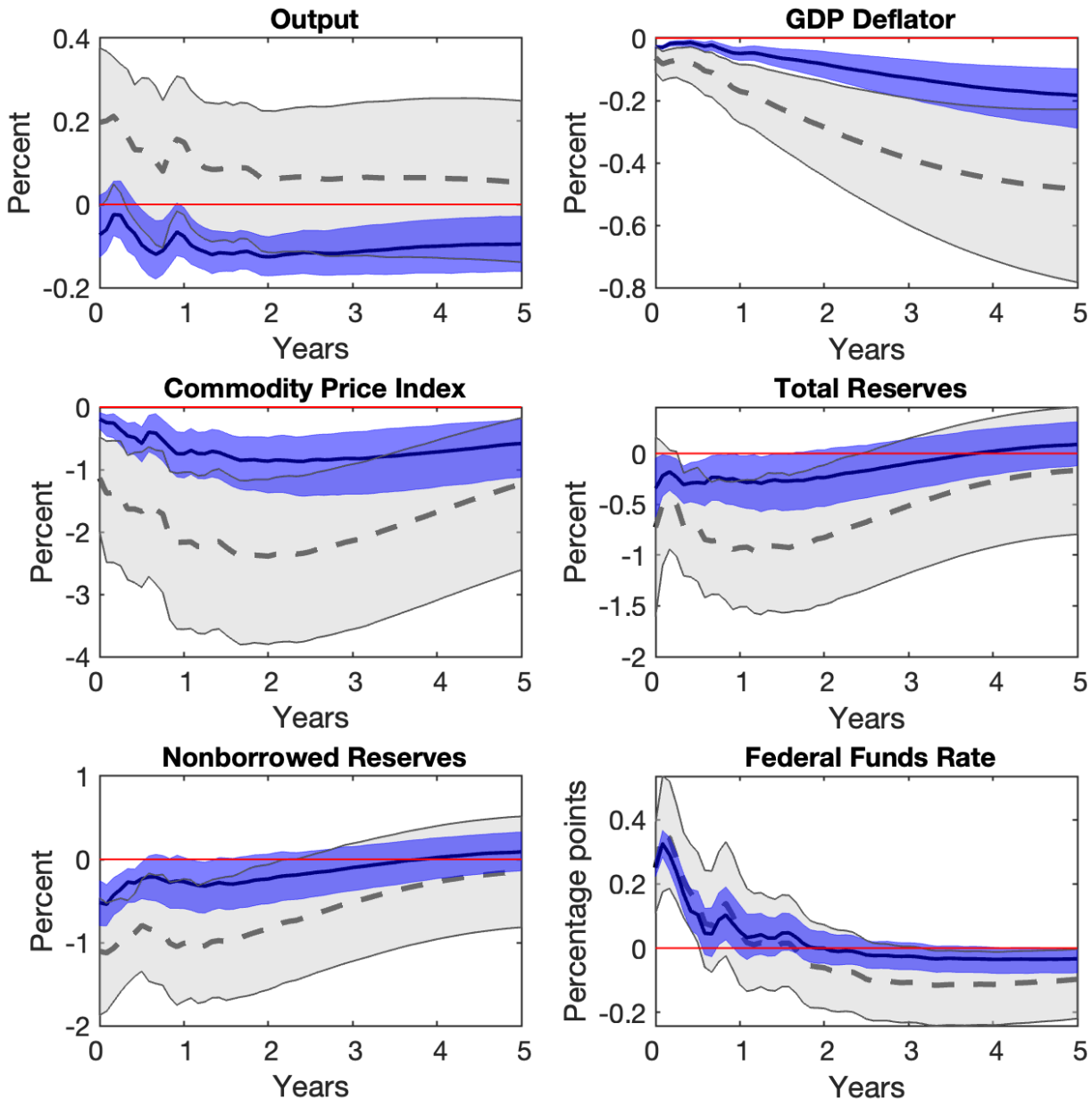

Figure 5: IRFs to a monetary policy shock (`Sign Restriction` 2 & `Matching Restriction` 2)

Notes: The lighter shaded areas and dashed lines are the 68 percent credible sets and the median IRFs, respectively, using `Sign Restriction` 2. The darker shaded areas and solid lines are the 68 percent credible sets and the median IRFs, respectively, using `Sign Restriction` 2 and `Matching Restriction` 2.

upper and lower bounds of posterior IRF samples compress substantially after `Matching Restriction` 2 is imposed, as in the previous application. We also present details of this exercise in Online Appendix D.

Finally, in Online Appendix F, we present the results when the narrative sign restrictions (as in Antolín-Díaz and Rubio-Ramírez, 2018), `Sign Restriction` 2, and `Matching Restriction` 2 are simultaneously imposed. Even when we consider the narrative sign restrictions, the results are not quantitatively different from those in this application. That is, the matching restriction allows output to react to a contractionary monetary policy shock more negatively and leads to narrower credible sets for the responses of all variables.

5 Conclusion

This paper introduces a novel identification scheme for SVARs, the matching restriction. This approach uses theoretical IRFs to define a prior over rotations, assigning higher prior density to rotations whose empirical IRF distributions are more compatible with the theoretical IRFs. We also derive the posterior distribution subject to both the sign restrictions and the matching restriction and describe the algorithm to draw the structural parameters from the distribution.

By applying this approach to two seminal monetary policy SVAR frameworks—Arias, Caldara, and Rubio-Ramírez (2019) and Uhlig (2005)—we demonstrate that the matching restriction provides a formal and systematic framework to incorporate the quantitative information from the theoretical model into SVAR identification. These SVARs are useful benchmarks because conventional sign-restriction approaches, albeit easy to implement, often leave long-standing anomalies unresolved, such as the price puzzle and the positive output response to a contractionary monetary policy shock.

Specifically, we impose a matching restriction based on the theoretical IRF of output in the SVAR of Arias, Caldara, and Rubio-Ramírez (2019), in which the price puzzle is present. Our results show that the matching restriction indeed resolves the price puzzle, even without matching price IRFs, by disciplining output dynamics toward theory. Similarly, we add a matching restriction based on the theoretical IRF of prices in the SVAR of Uhlig (2005), in which a contractionary monetary policy shock counterintuitively increases output. It is revealed that the matching restriction, even without matching output IRFs, allows the shock to depress output, consistent with theory.

Finally, while this study employs the matching restriction only in identifying monetary policy shocks, the matching restriction can be applied more broadly. It would be very promising to extend this restriction to identify other macroeconomic shocks, such as fiscal and technology shocks, for which theoretical IRFs are well-defined. Furthermore, the matching

restriction can be easily combined with other identification restrictions, such as zero or long-run restrictions. Since these issues are beyond the scope of our paper, we leave them for future research.

References

Antolín-Díaz, J. and J. F. Rubio-Ramírez (2018). Narrative sign restrictions for SVARs. *American Economic Review 108 (10)*, 2802–2829.

Arias, J. E., D. Caldara, and J. F. Rubio-Ramírez (2019). The systematic component of monetary policy in SVARs: An agnostic identification procedure. *Journal of Monetary Economics 101*, 1–13.

Arias, J. E., J. F. Rubio-Ramírez, and D. F. Waggoner (2018). Inference based on structural vector autoregressions identified with sign and zero restrictions: Theory and applications. *Econometrica 86 (2)*, 685–720.

Baumeister, C. and J. D. Hamilton (2015). Sign restrictions, structural vector autoregressions, and useful prior information. *Econometrica 83 (5)*, 1963–1999.

Baumeister, C. and J. D. Hamilton (2018). Inference in structural vector autoregressions when the identifying assumptions are not fully believed: Re-evaluating the role of monetary policy in economic fluctuations. *Journal of Monetary Economics 100*, 48–65.

Baumeister, C. and J. D. Hamilton (2024). Advances in using vector autoregressions to estimate structural magnitudes. *Econometric Theory 40 (3)*, 472–510.

Bernanke, B. S. and A. S. Blinder (1992). The federal funds rate and the channels of monetary transmission. *American Economic Review 82 (4)*, 901–921.

Bernanke, B. S., J. Boivin, and P. Eliasz (2005). Measuring the effects of monetary policy: A factor-augmented vector autoregressive (FAVAR) approach. *Quarterly Journal of Economics 120 (1)*, 387–422.

Canova, F. and M. Paustian (2011). Business cycle measurement with some theory. *Journal of Monetary Economics 58 (4)*, 345–361.

Christiano, L. J. and M. Eichenbaum (1992). Liquidity effects and the monetary transmission mechanism. *American Economic Review 82 (2)*, 346–353.

Christiano, L. J., M. Eichenbaum, and C. L. Evans (1996). The effects of monetary policy shocks: Evidence from the flow of funds. *Review of Economics and Statistics 78 (1)*, 16–34.

Christiano, L. J., M. Eichenbaum, and C. L. Evans (2005). Nominal rigidities and the dynamic effects of a shock to monetary policy. *Journal of Political Economy 113 (1)*, 1–45.

Christiano, L. J., M. Trabandt, and K. Walentin (2010). DSGE models for monetary policy analysis. In *Handbook of Monetary Economics*, Volume 3, pp. 285–367. Elsevier.

Cushman, D. O. and T. Zha (1997). Identifying monetary policy in a small open economy under flexible exchange rates. *Journal of Monetary Economics 39 (3)*, 433–448.

Del Negro, M. and F. Schorfheide (2004). Priors from general equilibrium models for VARs. *International Economic Review 45 (2)*, 643–673.

Fry, R. and A. Pagan (2011). Sign restrictions in structural vector autoregressions: A critical review. *Journal of Economic Literature 49 (4)*, 938–960.

Gertler, M. and P. Karadi (2015). Monetary policy surprises, credit costs, and economic activity. *American Economic Journal: Macroeconomics 7 (1)*, 44–76.

Giacomini, R. and T. Kitagawa (2021). Robust Bayesian inference for set-identified models. *Econometrica 89 (4)*, 1519–1556.

Jarociński, M. and P. Karadi (2020). Deconstructing monetary policy surprises—the role of information shocks. *American Economic Journal: Macroeconomics 12 (2)*, 1–43.

Kim, M. (2022). Transmission of U.S. monetary policy to commodity exporters and importers. *Review of Economic Dynamics 43*, 152–167.

Kleijn, B. and A. Van Der Vaart (2012). The Bernstein-Von-Mises theorem under misspecification. *Electronic Journal of Statistics 6*, 354–381.

Koop, G., D. J. Poirier, and J. L. Tobias (2007). *Bayesian Econometric Methods*. Number 7 in Econometric Exercises. Cambridge ; New York: Cambridge University Press.

Kuttner, K. N. (2001). Monetary policy surprises and interest rates: Evidence from the fed funds futures market. *Journal of Monetary Economics 47 (3)*, 523–544.

Liu, P. and K. Theodoridis (2012). DSGE model restrictions for structural VAR identification. *International Journal of Central Banking 8 (4)*, 61–95.

Lütkepohl, H. (1990). Asymptotic distributions of impulse response functions and forecast error variance decompositions of vector autoregressive models. *Review of Economics and Statistics 72 (1)*, 116–125.

Rigobon, R. and B. Sack (2004). The impact of monetary policy on asset prices. *Journal of Monetary Economics 51 (8)*, 1553–1575.

Romer, C. D. and D. H. Romer (1989). Does monetary policy matter? A new test in the spirit of Friedman and Schwartz. *NBER Macroeconomics Annual 4*, 121–170.

Romer, C. D. and D. H. Romer (2004). A new measure of monetary shocks: Derivation and implications. *American Economic Review 94 (4)*, 1055–1084.

Rubio-Ramírez, J. F., D. F. Waggoner, and T. Zha (2010). Structural vector autoregressions: Theory of identification and algorithms for inference. *Review of Economic Studies 77 (2)*, 665–696.

Rudebusch, G. D. (1998). Do measures of monetary policy in a VAR make sense? *International Economic Review 39 (4)*, 907–931.

Sims, C. A. (1992). Interpreting the macroeconomic time series facts: The effects of monetary policy. *European Economic Review 36 (5)*, 975–1000.

Smets, F. and R. Wouters (2007). Shocks and frictions in US business cycles: A Bayesian DSGE approach. *American Economic Review 97 (3)*, 586–606.

Strongin, S. (1995). The identification of monetary policy disturbances explaining the liquidity puzzle. *Journal of Monetary Economics 35 (3)*, 463–497.

Uhlig, H. (2005). What are the effects of monetary policy on output? Results from an agnostic identification procedure. *Journal of Monetary Economics 52 (2)*, 381–419.

Vaart, A. W. V. D. (1998). *Asymptotic Statistics*. Cambridge University Press.

Online Appendix for

"Identifying Monetary Policy Shocks by Matching Theoretical IRFs"

Myunghyun Kim* Sunho Lee† Inhwan So‡

Not for Publication

This appendix contains:

* Department of Economics, Sungkyunkwan University, Seoul, Korea (e-mail: mhkim7812@gmail.com).
† Bank of Korea, Seoul, Korea (e-mail: econ.preference@gmail.com).
‡ School of Economics, Hongik University, Seoul, Korea (e-mail: inhwanso@hongik.ac.kr).

A Asymptotic posterior distribution of empirical IRFs

This appendix derives the asymptotic posterior distribution of empirical IRFs conditional on a rotation $\mathbf{Q}$ (referred to as the $\mathbf{Q}$-conditional IRF distribution). This distribution is used to construct the theory-based prior over the rotation matrix for the matching restriction.

Let $\mathbf{Q} \in \mathcal{O}(n)$ be an $n \times n$ orthogonal matrix, where $\mathcal{O}(n) = \{\mathbf{Q} : \mathbf{Q}\mathbf{Q}' = \mathbf{I}_n\}$. Write $\mathbf{B}_1, \ldots, \mathbf{B}_p$ for the $n \times n$ lag-coefficient blocks in $\mathbf{B}'$, so that $\mathbf{B}' = [\mathbf{B}_1, \ldots, \mathbf{B}_p, \mathbf{b}_0]$, where $\mathbf{b}_0$ is the intercept block. Also, let $\mathbf{Y} = [\mathbf{Y}_1 \ \cdots \ \mathbf{Y}_T]'$ denote the sample. By the Bernstein-von Mises theorem, the posterior distribution of the reduced-form parameters is asymptotically normal under standard regularity conditions (Vaart, 1998; Kleijn and Van Der Vaart, 2012). Applied to the reduced-form representation, this implies the normal approximation as:

$$\begin{pmatrix} \text{vec}\left([\mathbf{B}_1, \ldots, \mathbf{B}_p]\right) \\ \text{vech}\left(\mathbf{\Sigma}\right) \end{pmatrix} \mid \mathbf{Y} \overset{a}{\sim} \mathcal{N}\left[\begin{pmatrix} \text{vec}\left([\overline{\mathbf{B}}_1, \ldots, \overline{\mathbf{B}}_p]\right) \\ \text{vech}\left(\overline{\mathbf{\Sigma}}\right) \end{pmatrix}, \mathbf{\Omega}_{B,\Sigma}^{post} \right], \tag{A.1}$$

where $\overline{\mathbf{B}}$ and $\overline{\mathbf{\Sigma}}$ are the posterior means of the reduced-form parameters, and $\mathbf{\Omega}_{B,\Sigma}^{post}$ is their posterior covariance matrix. Following Koop, Poirier, and Tobias (2007), we use posterior means and posterior covariances rather than the maximum-likelihood estimates and the inverse information matrix evaluated at the maximum-likelihood estimates. The asymptotic distribution based on posterior moments is closer to the finite-sample posterior distribution and retains the influence of the prior.[1]

To map the posterior distribution of the reduced-form parameters into the posterior distribution of empirical IRFs, we write the IRFs as functions of $(\mathbf{B}, \mathbf{\Sigma})$ and $\mathbf{Q}$. Given $(\mathbf{B}, \mathbf{\Sigma})$ and $\mathbf{Q}$, the rotated impact matrix $\mathbf{P}_Q(\mathbf{\Sigma})$ is defined as

$$\mathbf{P}_Q(\mathbf{\Sigma}) = R(\mathbf{\Sigma})' \mathbf{Q}, \tag{A.2}$$

where $R(\mathbf{\Sigma})$ is chosen to satisfy $R(\mathbf{\Sigma})' R(\mathbf{\Sigma}) = \mathbf{\Sigma}$. Then, the empirical IRF matrix conditional on $\mathbf{Q}$ is

$$\mathbf{IR}_h(\mathbf{B}, \mathbf{\Sigma}, \mathbf{Q}) = \mathbf{\Phi}_h(\mathbf{B}) \mathbf{P}_Q(\mathbf{\Sigma}), \qquad \text{for } h = 0, 1, \ldots, H-1, \tag{A.3}$$

where $\mathbf{\Phi}_h(\mathbf{B})$ denotes the $n \times n$ coefficient matrix at horizon h in the Wold moving-average representation of $\mathbf{Y}_t$, with $\mathbf{\Phi}_0(\mathbf{B}) = \mathbf{I}_n$. The stacked IRF vector across the matched horizons is

$$\mathbf{IR}(\mathbf{B}, \mathbf{\Sigma}, \mathbf{Q}) = \left(\text{vec}\left(\mathbf{IR}_0(\mathbf{B}, \mathbf{\Sigma}, \mathbf{Q})\right)', \ldots, \text{vec}\left(\mathbf{IR}_{H-1}(\mathbf{B}, \mathbf{\Sigma}, \mathbf{Q})\right)'\right)'.$$

[1] The latter feature is especially relevant when this procedure is applied to large Bayesian VARs, where the prior can substantially affect the reduced-form posterior.

In addition, the empirical IRF vector of the i-th variable to the k-th structural shock over the matched horizons conditional on $\mathbf{Q}$ is

$$\mathbf{IR}^{(i,k)}\left(\mathbf{B},\mathbf{\Sigma},\mathbf{Q}\right)=\mathbf{S}_{ik}\mathbf{IR}\left(\mathbf{B},\mathbf{\Sigma},\mathbf{Q}\right), \tag{A.4}$$

where $\mathbf{S}_{ik}$ is the selection matrix that extracts the (i,k)-th element of the stacked IRFs.

As shown by Lütkepohl (1990), applying the delta method to the result above with $\mathbf{Q}$ fixed yields the asymptotic distribution of the empirical IRF vector. To derive the derivatives for the delta method, we first express the Wold moving-average coefficient matrix $\mathbf{\Phi}_h\left(\mathbf{B}\right)$ in companion form as:

$$\mathbf{\Phi}_h\left(\mathbf{B}\right)=\mathbf{J}\mathcal{A}\left(\mathbf{B}\right)^h\mathbf{J}',$$

where $\mathcal{A}\left(\mathbf{B}\right)$ denotes the companion matrix composed of the reduced-form lag coefficients, and $\mathbf{J}=\begin{pmatrix}\mathbf{I}_n & \mathbf{0} & \cdots & \mathbf{0}\end{pmatrix}$ is the selection matrix. Following Lütkepohl (1990), the derivative of the coefficient $\mathbf{G}_h\left(\mathbf{B}\right)$ is given by:

$$\mathbf{G}_h\left(\mathbf{B}\right)=\frac{\partial\operatorname{vec}\left(\mathbf{\Phi}_h\left(\mathbf{B}\right)\right)}{\partial\operatorname{vec}\left(\left[\mathbf{B}_1,\ldots,\mathbf{B}_p\right]\right)'}=\sum_{\ell=0}^{h-1}\mathbf{J}\left(\mathcal{A}\left(\mathbf{B}\right)'\right)^{h-1-\ell}\otimes\mathbf{\Phi}_\ell\left(\mathbf{B}\right),\qquad\text{for } h\geq 1,$$

with $\mathbf{G}_0\left(\mathbf{B}\right)=\mathbf{0}$. Using Equation (A.2), we differentiate the impact matrix $\mathbf{P}_Q\left(\mathbf{\Sigma}\right)$ as:

$$\mathbf{H}_Q\left(\mathbf{\Sigma}\right)=\frac{\partial\operatorname{vec}\left(\mathbf{P}_Q\left(\mathbf{\Sigma}\right)\right)}{\partial\operatorname{vech}\left(\mathbf{\Sigma}\right)'}=\left(\mathbf{Q}'\otimes\mathbf{I}_n\right)\mathbf{H}_0\left(\mathbf{\Sigma}\right),$$

with $\mathbf{H}_0\left(\mathbf{\Sigma}\right)=\partial\operatorname{vec}\left(R\left(\mathbf{\Sigma}\right)'\right)/\partial\operatorname{vech}\left(\mathbf{\Sigma}\right)'$. In this paper, we use the Cholesky decomposition for $R\left(\mathbf{\Sigma}\right)$. When $R\left(\mathbf{\Sigma}\right)$ is specified using the Cholesky decomposition, Lütkepohl (1990) shows that $\mathbf{H}_0\left(\mathbf{\Sigma}\right)$ can be explicitly evaluated as:

$$\mathbf{H}_0\left(\mathbf{\Sigma}\right)=\mathbf{L}_n'\left[\mathbf{L}_n\left(\mathbf{I}_{n^2}+\mathbf{K}_{nn}\right)\left(R\left(\mathbf{\Sigma}\right)'\otimes\mathbf{I}_n\right)\mathbf{L}_n'\right]^{-1},$$

where $\mathbf{L}_n$ is the elimination matrix such that $\operatorname{vech}(\mathbf{M})=\mathbf{L}_n\operatorname{vec}(\mathbf{M})$ for any $n\times n$ matrix $\mathbf{M}$, and $\mathbf{K}_{nn}$ is the commutation matrix such that $\mathbf{K}_{nn}\operatorname{vec}(\mathbf{M})=\operatorname{vec}(\mathbf{M}')$.

We now differentiate the empirical IRFs with respect to the reduced-form parameters. From Equation (A.3), the vectorization of the empirical IRF matrix at horizon h can be rearranged as:

$$\operatorname{vec}\left(\mathbf{IR}_h\left(\mathbf{B},\mathbf{\Sigma},\mathbf{Q}\right)\right)=\left(\mathbf{P}_Q\left(\mathbf{\Sigma}\right)'\otimes\mathbf{I}_n\right)\operatorname{vec}\left(\mathbf{\Phi}_h\left(\mathbf{B}\right)\right).$$

Then, its derivative with respect to the lag coefficients yields:

$$\mathbf{C}_{h,B}\left(\mathbf{B},\mathbf{\Sigma},\mathbf{Q}\right)=\frac{\partial\operatorname{vec}\left(\mathbf{IR}_h\left(\mathbf{B},\mathbf{\Sigma},\mathbf{Q}\right)\right)}{\partial\operatorname{vec}\left(\left[\mathbf{B}_1,\ldots,\mathbf{B}_p\right]\right)'}=\left(\mathbf{P}_Q\left(\mathbf{\Sigma}\right)'\otimes\mathbf{I}_n\right)\mathbf{G}_h\left(\mathbf{B}\right).$$

Similarly, to evaluate the derivative with respect to the covariance parameters, we reformulate the vectorization of the empirical IRF matrix as:

$$\operatorname{vec}\left(\mathbf{IR}_h\left(\mathbf{B},\mathbf{\Sigma},\mathbf{Q}\right)\right)=\left(\mathbf{I}_n\otimes\mathbf{\Phi}_h\left(\mathbf{B}\right)\right)\operatorname{vec}\left(\mathbf{P}_Q\left(\mathbf{\Sigma}\right)\right).$$

Hence, its derivative with respect to $\operatorname{vech}\left(\mathbf{\Sigma}\right)$ yields:

$$\mathbf{C}_{h,\Sigma}\left(\mathbf{B},\mathbf{\Sigma},\mathbf{Q}\right)=\frac{\partial\operatorname{vec}\left(\mathbf{IR}_h\left(\mathbf{B},\mathbf{\Sigma},\mathbf{Q}\right)\right)}{\partial\operatorname{vech}\left(\mathbf{\Sigma}\right)'}=\left(\mathbf{I}_n\otimes\mathbf{\Phi}_h\left(\mathbf{B}\right)\right)\mathbf{H}_Q\left(\mathbf{\Sigma}\right).$$

The horizon-specific Jacobian of $\operatorname{vec}\left(\mathbf{IR}_h\left(\mathbf{B},\mathbf{\Sigma},\mathbf{Q}\right)\right)$ is then

$$\mathbf{C}_h\left(\mathbf{B},\mathbf{\Sigma},\mathbf{Q}\right)=\left[\mathbf{C}_{h,B}\left(\mathbf{B},\mathbf{\Sigma},\mathbf{Q}\right),\mathbf{C}_{h,\Sigma}\left(\mathbf{B},\mathbf{\Sigma},\mathbf{Q}\right)\right].$$

The intercept block does not enter the IRF mapping; equivalently, the columns of the IRF Jacobian corresponding to the constant terms are set to zero, and are thus omitted from $\mathbf{C}_h\left(\mathbf{B},\mathbf{\Sigma},\mathbf{Q}\right)$. Stacking the derivative matrices over the horizons, we construct the full Jacobian matrix as:

$$\mathbf{C}\left(\mathbf{B},\mathbf{\Sigma},\mathbf{Q}\right)=\left(\mathbf{C}_0\left(\mathbf{B},\mathbf{\Sigma},\mathbf{Q}\right)',\mathbf{C}_1\left(\mathbf{B},\mathbf{\Sigma},\mathbf{Q}\right)',\ldots,\mathbf{C}_{H-1}\left(\mathbf{B},\mathbf{\Sigma},\mathbf{Q}\right)'\right)'.$$

Finally, applying the delta method to Equations (A.1) and (A.4) gives the $\mathbf{Q}$-conditional IRF distribution:

$$\begin{aligned}&\mathbf{IR}^{(i,k)}\mid\mathbf{Y},\mathbf{Q}\overset{a}{\sim}\mathcal{N}\left(\boldsymbol{\mu}_Q^{(i,k)}\left(\mathbf{Y}\right),\mathbf{V}_Q^{(i,k)}\left(\mathbf{Y}\right)\right)\\ \text{with }&\boldsymbol{\mu}_Q^{(i,k)}\left(\mathbf{Y}\right)=\mathbf{S}_{ik}\mathbf{IR}\left(\overline{\mathbf{B}},\overline{\mathbf{\Sigma}},\mathbf{Q}\right)\\ \text{and }&\mathbf{V}_Q^{(i,k)}\left(\mathbf{Y}\right)=\mathbf{S}_{ik}\mathbf{C}\left(\overline{\mathbf{B}},\overline{\mathbf{\Sigma}},\mathbf{Q}\right)\mathbf{\Omega}_{B,\Sigma}^{post}\mathbf{C}\left(\overline{\mathbf{B}},\overline{\mathbf{\Sigma}},\mathbf{Q}\right)'\mathbf{S}_{ik}'.\end{aligned}\tag{A.5}$$

B Parameter values for the New Keynesian DSGE model

The values of the parameters in the New Keynesian DSGE model are listed in Table B. Specifically, one period in the model is one quarter, and all the parameter values are borrowed from Christiano, Eichenbaum, and Evans (2005) and Smets and Wouters (2007). Note that, since we are interested in monetary policy shocks only, we do not assign values to the parameters associated with other exogenous variables.

Table B: Parameter values for the New Keynesian DSGE model

Parameter	Value	Source
β	$1.03^{-0.25}$	Christiano, Eichenbaum, and Evans (2005)
δ	0.025	Christiano, Eichenbaum, and Evans (2005)
α	0.36	Christiano, Eichenbaum, and Evans (2005)
b	0.7	Smets and Wouters (2007)
τ	5.7	Smets and Wouters (2007)
$\varepsilon_p = \varepsilon_w$	10	Smets and Wouters (2007)
χ	1.9	Smets and Wouters (2007)
θ_p	0.66	Smets and Wouters (2007)
θ_w	0.73	Smets and Wouters (2007)
ρ_i	0.8	Smets and Wouters (2007)
ϕ_π	2	Smets and Wouters (2007)
ϕ_y	0.2	Smets and Wouters (2007)
ω^g	0.18	Smets and Wouters (2007)

C Frequency alignment and shock normalization

To apply the matching restriction, the theoretical and empirical IRFs should be expressed at the same frequency, and the shocks in the SVAR and DSGE models should be normalized. However, most DSGE models assume a quarterly frequency, while most SVARs for monetary policy analysis are estimated with monthly data. Furthermore, in our monetary policy applications, a contractionary monetary policy shock should raise the federal funds rate by 25 basis points on impact, as assumed in the DSGE model. To incorporate these two adjustments jointly into the matching kernel, we derive the adjusted moments of the $\mathbf{Q}$-conditional IRF distribution, denoted by $\widetilde{\boldsymbol{\mu}}_Q^{(i,k)}(\mathbf{Y})$ and $\widetilde{\mathbf{V}}_Q^{(i,k)}(\mathbf{Y})$.

(i) $\widetilde{\boldsymbol{\mu}}_Q^{(i,k)}(\mathbf{Y})$: If the theoretical IRF is quarterly and the empirical IRF is monthly, define the normalized quarterly empirical IRF function by

$$\widetilde{IR}_q^{(i,k)}(\mathbf{B},\boldsymbol{\Sigma},\mathbf{Q}) = 0.25 \cdot \frac{1}{3}\sum_{m=3q}^{3q+2} \frac{IR_m^{(i,k)}(\mathbf{B},\boldsymbol{\Sigma},\mathbf{Q})}{IR_0^{(j,k)}(\mathbf{B},\boldsymbol{\Sigma},\mathbf{Q})}, \qquad q = 0,\ldots,H-1, \tag{C.1}$$

where j denotes the index of the policy-rate variable in $\mathbf{Y}_t$, and $IR_m^{(a,b)}(\mathbf{B},\mathbf{\Sigma},\mathbf{Q})$ represents the (a,b)-th element of $\mathbf{IR}_m(\mathbf{B},\mathbf{\Sigma},\mathbf{Q})$. The denominator is the impact response of the policy-rate variable to the k-th shock, which is the monetary policy shock in our applications. This definition first scales the empirical IRF by the policy-rate impact response, then averages the three monthly responses in each quarter, and finally multiplies the result by 0.25 to express the IRF as the response to a 25-bp policy-rate increase. The transformed mean used in the matching kernel is obtained by evaluating this function at the posterior means:

$$\widetilde{\boldsymbol{\mu}}_Q^{(i,k)}(\mathbf{Y}) = \left(\widetilde{IR}_0^{(i,k)}(\overline{\mathbf{B}},\overline{\mathbf{\Sigma}},\mathbf{Q}), \widetilde{IR}_1^{(i,k)}(\overline{\mathbf{B}},\overline{\mathbf{\Sigma}},\mathbf{Q}), \ldots, \widetilde{IR}_{H-1}^{(i,k)}(\overline{\mathbf{B}},\overline{\mathbf{\Sigma}},\mathbf{Q})\right)'.$$

(ii) $\widetilde{\mathbf{V}}_Q^{(i,k)}(\mathbf{Y})$: The delta-method covariance used in the matching kernel is obtained by differentiating the normalized quarterly IRF function in Equation (C.1). Let $\mathbf{C}_m^{(a,b)}(\mathbf{B},\mathbf{\Sigma},\mathbf{Q})$ denote the row vector of the monthly IRF Jacobian corresponding to $IR_m^{(a,b)}(\mathbf{B},\mathbf{\Sigma},\mathbf{Q})$, equivalently, the $(m+1)$-th row of $\mathbf{S}_{ab}\mathbf{C}(\mathbf{B},\mathbf{\Sigma},\mathbf{Q})$. The q-th row of the transformed Jacobian is

$$\widetilde{\mathbf{C}}_{Q,q}^{(i,k)}(\mathbf{Y}) = 0.25 \cdot \frac{1}{3}\sum_{m=3q}^{3q+2}\left[\frac{\mathbf{C}_m^{(i,k)}(\overline{\mathbf{B}},\overline{\mathbf{\Sigma}},\mathbf{Q})}{IR_0^{(j,k)}(\overline{\mathbf{B}},\overline{\mathbf{\Sigma}},\mathbf{Q})} - \frac{IR_m^{(i,k)}(\overline{\mathbf{B}},\overline{\mathbf{\Sigma}},\mathbf{Q})\mathbf{C}_0^{(j,k)}(\overline{\mathbf{B}},\overline{\mathbf{\Sigma}},\mathbf{Q})}{\left[IR_0^{(j,k)}(\overline{\mathbf{B}},\overline{\mathbf{\Sigma}},\mathbf{Q})\right]^2}\right].$$

Stacking these rows gives $\widetilde{\mathbf{C}}_Q^{(i,k)}(\mathbf{Y})$. Then, the covariance matrix is

$$\widetilde{\mathbf{V}}_Q^{(i,k)}(\mathbf{Y}) = \widetilde{\mathbf{C}}_Q^{(i,k)}(\mathbf{Y})\mathbf{\Omega}_{B,\Sigma}^{post}\widetilde{\mathbf{C}}_Q^{(i,k)}(\mathbf{Y})'.$$

The diagonal matrix $\widetilde{\mathbf{D}}_Q^{(i,k)}(\mathbf{Y})$ used in the kernel is obtained by retaining only the diagonal elements of $\widetilde{\mathbf{V}}_Q^{(i,k)}(\mathbf{Y})$.

Finally, the matching kernel used in applications with different frequencies is

$$m(\mathbf{Q};\mathbf{Y}) = \phi_H\left[\mathbb{IR}^{(i,k)}; \widetilde{\boldsymbol{\mu}}_Q^{(i,k)}(\mathbf{Y}), \widetilde{\mathbf{D}}_Q^{(i,k)}(\mathbf{Y})\right]. \tag{C.2}$$

D Posterior IRF bounds and identification uncertainty

Uncertainty in set-identified SVARs can be decomposed into two components: (i) estimation uncertainty and (ii) identification uncertainty. Estimation uncertainty arises from the finite-sample noise in the reduced-form parameters, which are updated by the data. In contrast, identification uncertainty originates from the non-unique rotation matrix, whose conditional

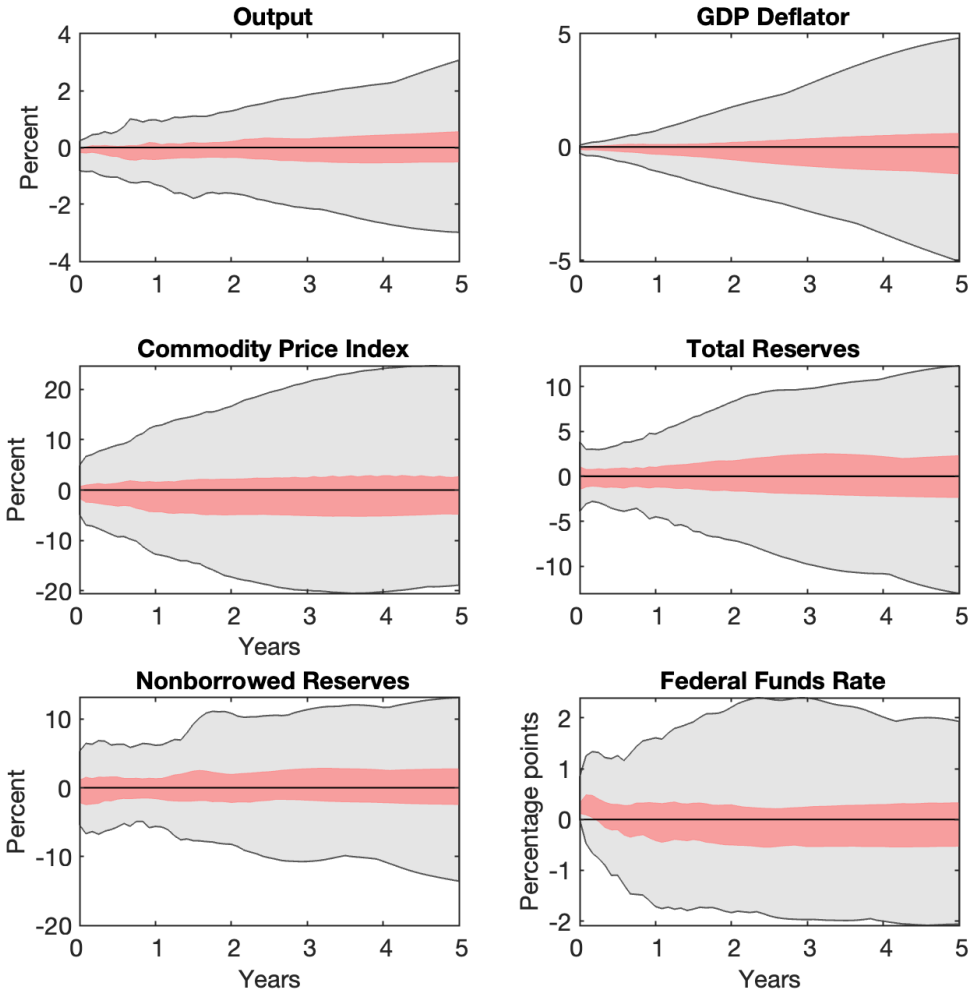

Figure D.1: Upper and lower bounds of posterior IRF samples
(`Sign Restriction` 1 & `Matching Restriction` 1)

Notes: The figure plots the areas between the lower and upper bounds of the posterior IRF samples. The lighter shaded areas correspond to `Sign Restriction` 1 alone, and the darker (red) shaded areas correspond to the posterior sample obtained after applying `Sign Restriction` 1 and `Matching Restriction` 1.

prior given the reduced-form parameters is not updated by the data.[2]

Because the matching restriction does not alter the reduced-form likelihood and prior and operates through the prior over rotations, compression of the posterior IRF distribution after imposing the matching restriction mainly reflects a reduction in identification uncertainty over the rotation matrix. Therefore, this appendix reports the upper and lower bounds of posterior IRF samples to visualize how much the matching restriction compresses this source of uncertainty. If the matching restriction substantially reduces identification uncertainty, these bounds should become significantly narrower after imposing the restriction.[3]

[2] Giacomini and Kitagawa (2021) refer to these as the revisable and unrevisable components of the prior, respectively.

[3] Another way to show identification uncertainty is to use the robust Bayesian framework of Giacomini and Kitagawa (2021). To reflect identification uncertainty, their framework derives the upper and lower

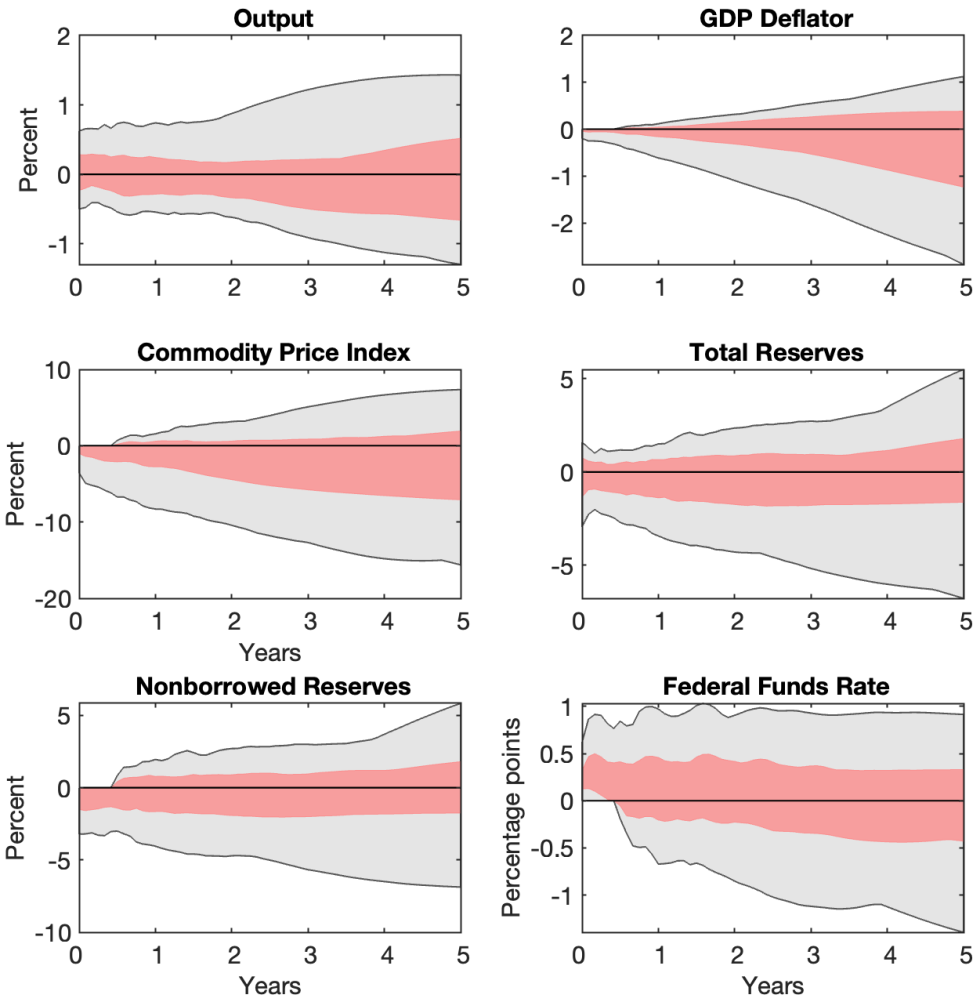

Figure D.2: Upper and lower bounds of posterior IRF samples
(`Sign Restriction` 2 & `Matching Restriction` 2)

Notes: The figure plots the areas between the lower and upper bounds of the posterior IRF samples. The lighter shaded areas correspond to `Sign Restriction` 2 alone, and the darker (red) shaded areas correspond to the posterior sample obtained after applying `Sign Restriction` 2 and `Matching Restriction` 2.

Figures D.1 and D.2 plot these bounds for the IRFs to a contractionary monetary policy shock. The gray shaded areas represent the upper and lower bounds under only the sign restrictions, while the red shaded areas show the bounds after incorporating the matching restriction. The bounds are consistently far more compressed after applying the matching restriction, which implies that the matching restriction substantially reduces identification uncertainty associated with the rotation matrix.

bounds of posterior means that can be obtained across alternative priors over the rotation matrix, without committing to a single prior over admissible rotations. In contrast, our matching restriction explicitly specifies a prior density over rotations, making the robust Bayesian framework difficult to apply directly. For this reason, instead of applying the robust Bayesian framework, we report the maximum and minimum values of the posterior IRF samples at each horizon before and after applying the matching prior. This comparison visualizes the reduction in identification uncertainty.

E Adding zero restrictions to Section 4.2

In this appendix, we additionally incorporate the zero restrictions used in Arias, Caldara, and Rubio-Ramírez (2019) into the SVAR model in Section 4.2. By doing so, this exercise further examines whether the matching restriction is still effective in the identification of monetary policy shocks when combined with short-run restrictions. Specifically, the zero restrictions are given as

Zero Restriction 1: *The federal funds rate reacts contemporaneously only to output, prices, and commodity prices.*

`Zero restriction` 1 implies that the federal funds rate does not contemporaneously react to total and nonborrowed reserves. That is, the two contemporaneous reserves are not included in the equation for the federal funds rate. This restriction is added to the two identification schemes employed in Section 4.2: (i) `Sign Restriction` 1 alone and (ii) `Sign Restriction` 1 and `Matching Restriction` 1.

Figure E depicts the IRFs of the variables to a contractionary monetary policy shock. The empirical IRFs under `Sign Restriction` 1 and `Zero Restriction` 1 are computed from 399,201 draws, and they are resampled to incorporate `Matching Restriction` 1.[4] As Figure E shows, the key message remains similar to the baseline results in Figure 3 in the main text, although the responses of total reserves and nonborrowed reserves, to which the zero restrictions are directly applied, display somewhat different patterns. The inclusion of `Zero Restriction` 1 does not yield a significant difference from the results with only the sign restrictions. Notably, even with the additional zero restrictions, the price puzzle persists.

However, once `Matching Restriction` 1 is incorporated, the identification of monetary policy shocks is substantially sharpened. Specifically, the price puzzle effectively disappears, and the IRFs of key macroeconomic variables become noticeably more distinct. This demonstrates that, unlike standard short-run zero restrictions that may lack sufficient information to resolve empirical anomalies, the matching restriction serves as a useful complementary tool.

[4] The effective sample size implied by the importance weights is 1,106.2. The largest normalized weight is 0.37%.

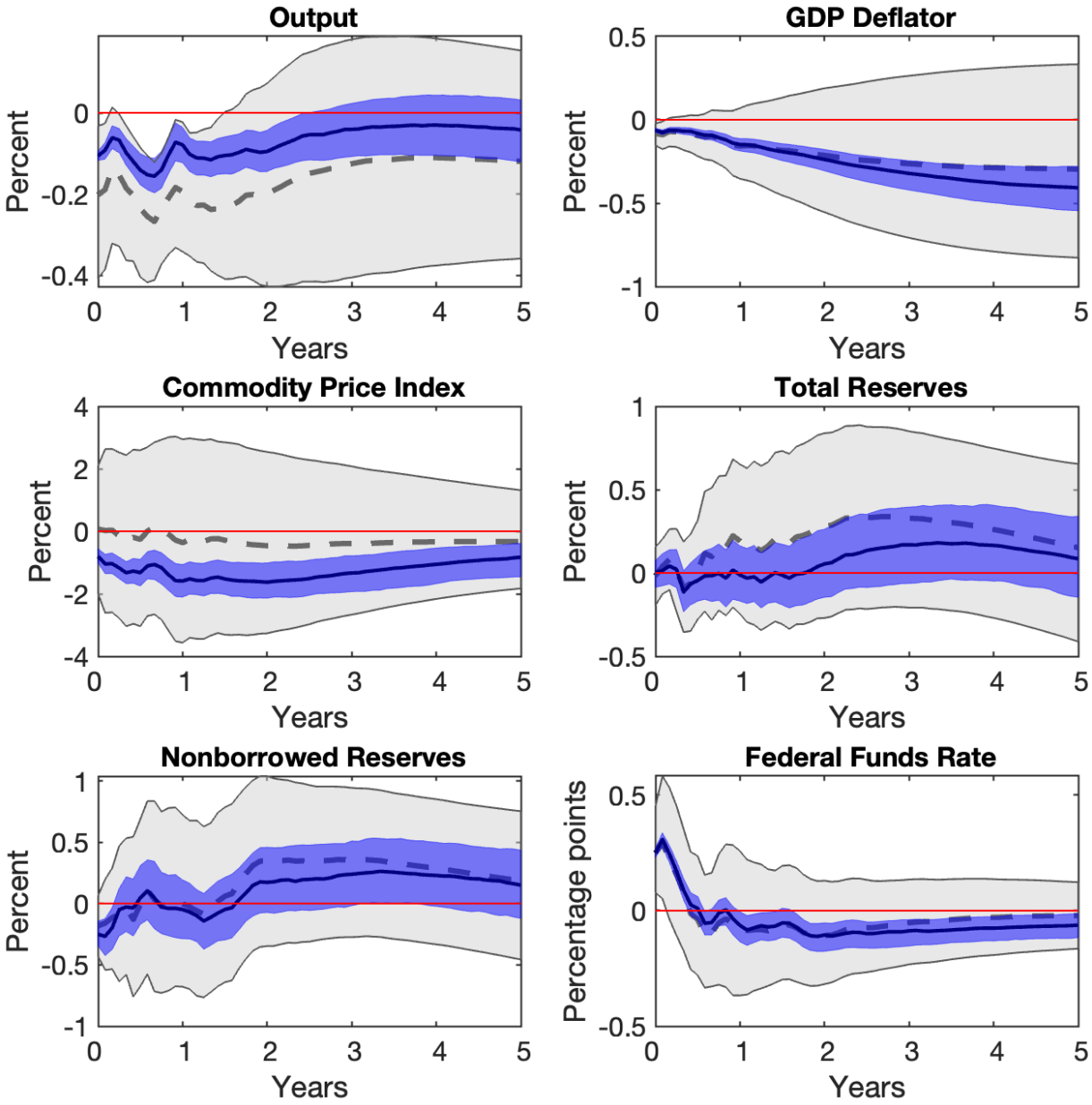

Figure E: IRFs to a monetary policy shock
(`Sign Restriction 1`, `Zero Restriction 1`, and `Matching Restriction 1`)

Notes: The lighter shaded areas and dashed lines are the 68 percent credible sets and the median IRFs, respectively, using `Sign Restriction 1` and `Zero restriction 1`. The darker shaded areas and solid lines are the 68 percent credible sets and the median IRFs, respectively, using `Sign Restriction 1`, `Zero restriction 1`, and `Matching Restriction 1`.

F Adding narrative sign restrictions to Section 4.3

In this appendix, we further extend the robustness check by incorporating the narrative sign restrictions employed by Antolín-Díaz and Rubio-Ramírez (2018) into the SVAR framework of Section 4.3. Narrative sign restrictions incorporate historical information about specific episodes into the identification. The specific narrative sign restriction that we impose is

Narrative Sign Restriction 1: *The monetary policy shock for the observation corresponding to October 1979 must be positive. In addition, for this observation, the absolute contribution of the monetary policy shock to the unexpected movement in the federal funds rate must be larger than the sum of the absolute contributions of all other structural shocks.*

The IRFs of the variables to a contractionary monetary policy shock are displayed in Figure F. The empirical IRFs under `Sign Restriction` 2 and `Narrative Sign Restriction` 1 are computed from 67,444 draws, and these draws are resampled to incorporate `Matching Restriction` 2.[5] As shown in Antolín-Díaz and Rubio-Ramírez (2018), the inclusion of narrative sign restrictions leads to a substantial improvement in identifying the structural effects of monetary policy shocks compared to the baseline case with only the sign restrictions. Specifically, under `Sign Restriction` 2 and `Narrative Sign Restriction` 1, the output response—which is positive under `Sign Restriction` 2 alone—becomes distinctly negative around 14 months after the shock. These results suggest that the narrative information regarding the Volcker disinflation period is useful in identifying the monetary policy shocks.

When `Matching Restriction` 2 is further imposed together with `Sign Restriction` 2 and `Narrative Sign Restriction` 1, output decreases more, and the credible set for the output IRF becomes tighter. Moreover, the credible sets for the IRFs of other variables are, by and large, narrower than those under `Sign Restriction` 2 and `Narrative Sign Restriction` 1. These results clearly suggest that the matching restriction acts as a complementary tool in the identification of monetary policy shocks even when the narrative restrictions are imposed.

[5] The effective sample size implied by the importance weights is 1,192.3. The largest normalized weight is 0.41%.

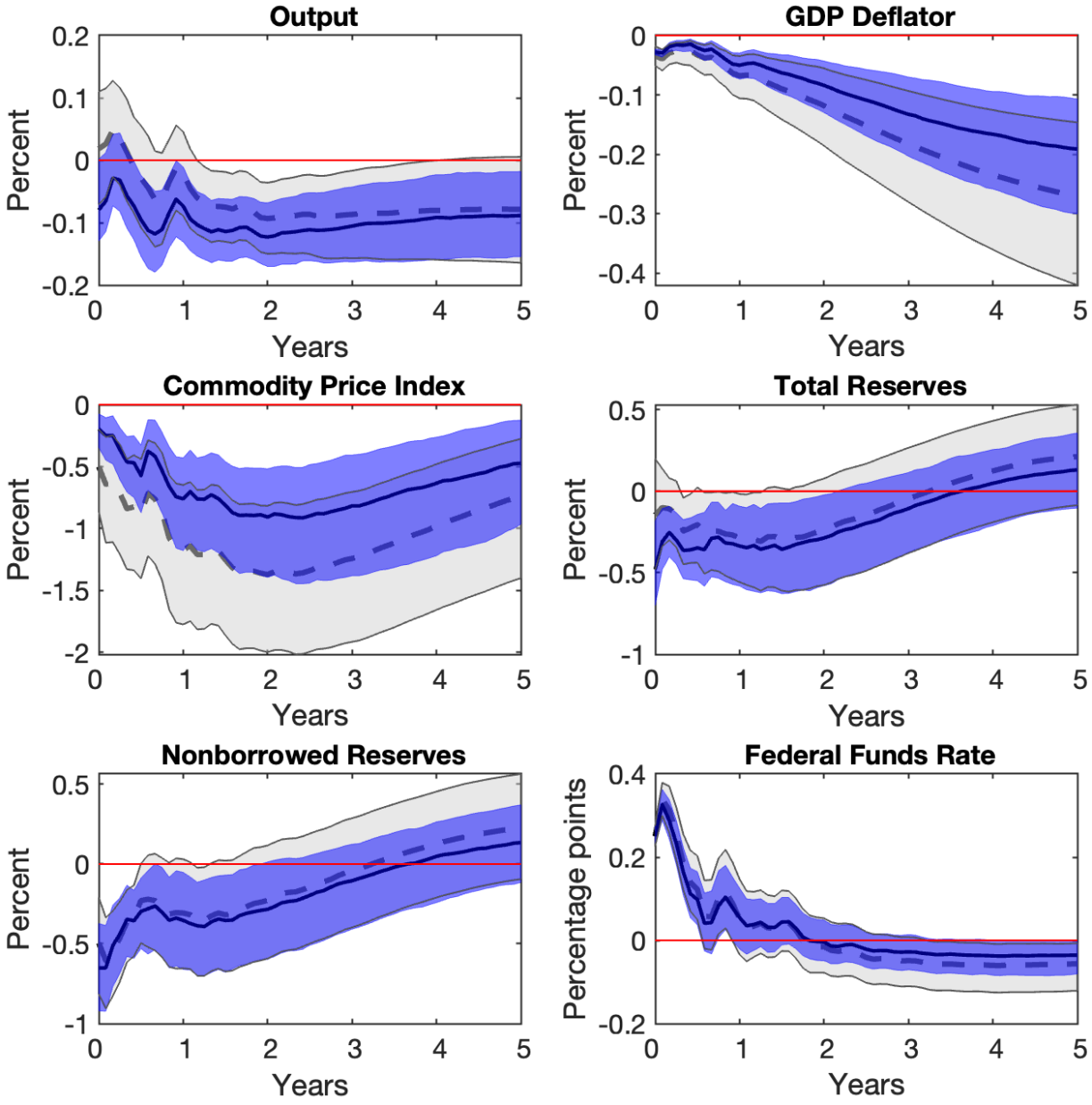

Figure F: IRFs to a monetary policy shock
(`Sign Restriction 2`, `Narrative Sign Restriction 1`, and `Matching Restriction 2`)

Notes: The lighter shaded areas and dashed lines are the 68 percent credible sets and the median IRFs, respectively, using `Sign Restriction 2` and `Narrative Sign Restriction 1`. The darker shaded areas and solid lines are the 68 percent credible sets and the median IRFs, respectively, using `Sign Restriction 2`, `Narrative Sign Restriction 1`, and `Matching Restriction 2`.